Article

Analytical investigation of effects of secondary structural members on the structural behaviors of transmission towers

Pyounghwa Kim [1], Whi Seok Han [1], Jeong Hun Kim [2], Jeonghwa Lee [3], Young Jong Kang [1], Seungjun Kim [1,*]

[1] School of Civil, Environmental, and Architectural Engineering, Korea University, Seoul 02841, Korea; kph2008@korea.ac.kr (P.K.); headdong27@korea.ac.kr (W.S.H.); yjkang@korea.ac.kr (Y.J.K.)
[2] Next Generation Transmission & Substation Lab., KEPCO Research Institute, Daejeon, Korea; jhkim78@kepco.co.kr (J.H.K.)
[3] Future and Fusion Lab of Architectural, Civil and Environmental Engineering (F-ACE Lab), Korea University, Seoul 02841, Korea; qevno@korea.ac.kr (J.L.)
* Correspondence: rocksmell@korea.ac.kr, Tel: +82-2-3290-4868

Abstract: A high-voltage transmission tower consists of structures to avoid the risk of electric shock and to prevent the risk of collapse. Hence, towers are generally designed to be high-rise for efficiency. The main posts of the tower are primary structural members that resist loads under various load conditions. Therefore, the contribution of the secondary member to securing the stiffness and strength of the main posts by reducing the effective buckling length is important. However, there are no detailed design criteria for secondary members. In this study, the structural effects of horizontal members and braces on the torsional stiffness, elastic buckling strength, and load-carrying capacity of transmission towers were observed through various structural analysis methods including linear-elastic, eigenvalue, and geometric nonlinear and inelastic analyses under governing load combinations. According to the analytical study, rather than the horizontal members, the brace spacing significantly affects the structural performance. Therefore, the number of horizontal members can be minimized if sufficient brace members are erected. If the brace spacing is wide, it is recommended that the horizontal members be erected to create K bracing, and the buckling resistance of the main posts can be thus enhanced.

Keywords: high-rise transmission tower; secondary structural members; brace, horizontal member; load-carrying capacity; geometry simplification

1. Introduction

Transmission towers are essential for transmitting large amounts of energy to decentralized areas. As the energy demand increases, high-capacity transmission towers are required. Accordingly, as the capacity of the transmission tower increases, the size of the structure increases as well. To ensure safety of the transmission tower, many secondary members are installed, which increases maintenance costs. If only structural safety is secured, the removal of excess members is necessary. Therefore, a design that considers the structural safety and cost aspects of maintenance is required.

A transmission tower resists various load conditions: the load combinations are explained in the ASCE 74 [1]. Many researchers have conducted structural safety studies on transmission towers under various load conditions [2–8]. In particular, various studies have been conducted on wind loads [9–17].

The transmission tower is a steel structure composed of a main post to resist the main loads applied to the tower body and an auxiliary member to support the main post. The auxiliary member consists of the horizontal member and braces. For the conventional lattice structures, the horizontal members and braces are expected to maintain the distance between the main post and reduce the effective buckling length. It also serves to prevent twisting of the constituting shape. Transmission towers are vulnerable to buckling under external loads owing to the characteristics of the steel structures. Hence, many studies on

 doi:10.20944/preprints202212.0129.v1

the buckling of trans-mission towers have been conducted [18,19]. Zhang et al. [20] described the importance of preventing buckling by identifying the risk of buckling and the diagonal members that are vulnerable to buckling.

Albermani et al. [21] conducted a study to improve the load-carrying capacity of a transmission tower by reinforcing the horizontal members. Albermani et al. [22] conducted a study to increase the load-carrying capacity of an existing transmission tower, using horizontal members of various shapes, and verified that the load-carrying capacity increased. In addition, several scholars have described the effects of the horizontal member in enhancing the overall load-carrying capacity of the transmission tower [18, 19, 21, 23–28]. The structural stability of the transmission tower can be achieved by enhancing the stiffness of the horizontal and brace members. Furthermore, many researchers have simplified the braces of transmission towers using various techniques [29–36].

As the height of the transmission tower is enlarged, the dimension of the main post is also required to increase due to the increased external loads. In Korea, nowadays the circular pipe section members are designed for the large-scale transmission tower in order to enhance buckling resistance. In means that the research to suggest the rational design of the secondary members for the new type transmission tower should be conducted because the previous studies have been undertaken for towers with slender angle section members. In fact, the description of the position or shape of the horizontal and brace members is only briefly explained or not presented in ASCE 10-15 (Design of Latticed Steel Transmission Structures) [37]. Therefore, the study of the effects of the secondary members on the structural behaviors of the large-scale transmission tower should be investigated.

In this study, the effect of secondary members on the structural response of transmission towers was analyzed. The parameters were the presence of horizontal members, spacing, and shape of the braces. The displacement and distorted shape due to torsional loads generated by broken wires were analyzed in the linear static analysis, and the contribution of the secondary members to the results was confirmed. In the eigenvalue analysis under wind load conditions, which is the governing condition of the transmission tower, an effect of the secondary members on the buckling strength of the main post was observed, by reducing the effective buckling length. Geometric nonlinear and inelastic analysis was conducted to confirm the effect of secondary members on the load-carrying capacity. By observing the load–displacement curves of the tower under the wind load condition, the effects of the secondary member parameters on the ultimate state were confirmed analytically.

2. General configuration and design load combinations for the transmission towers

2.1 Description and characteristics of the structures

2.1.1 Details of the model

A 765 kV-class lattice tower provided by Korea Eleetric Power Corporation was studied. This 109-m high tower was structured with equal-legged angles. As the capacity increased, a higher load was applied to the transmission tower. The cross-section of the main post changed from angular sections to hollow circular sections. The upper frame of the model was composed of 3.80 m × 3.80 m square, and the lower frame was composed of 19.62 m × 19.62 m square. The lattice transmission tower supported two cross-arms at the top of the tower for the ground wires and two arms comprising three layers to support the electric power lines (conductors). The model shape is shown in Fig. 1. Fig. 2 shows the wind direction along the transmission line.

The examined lattice transmission tower consists of two types of members: angle members and circular pipe section members. The cross-arm is composed of an angle section member, and the main post, braces, and horizontal member are composed of a circular pipe section member. The details of the members are shown in Fig. 3. Sixteen angle members and fifteen circular pipe section members were used to design the section members. The yield strengths of the circular pipe section and angle section were 345 and 290 MPa, respectively to perform geometric nonlinear and inelastic analysis by applying a

Preprints (www.preprints.org) | NOT PEER-REVIEWED | Posted: 7 December 2022 doi:10.20944/preprints202212.0129.v1

bilinear elastic-plastic model. The steel material properties are a mass density ϱ = 7,850 kg/m3, Young's modulus E = 210 GPa, and Poisson's ratio ν = 0.3. Table 1 summarizes the section properties of the 765-kV transmission tower.

The horizontal angle of the wire was 30°, and the wind span and weight span were 450 and 800 m, respectively. For conductors, the cardinal aluminum conductor steel-reinforced model, primarily used in 765 kV-class lattice transmission towers, was applied. The rated tensile strength was 150 kN, and the unit weight was 17.26 N/m. The rated tensile strength of the ground wire, AWS-200, was 126 kN, and the unit weight was 9.42 N/m. Table 2 summarizes the properties of the conductors and the ground wire.

The transmission tower consists of three parts: (a) common part, (b) body part, and (c) leg part. This study focused on the body parts of the transmission towers. Changes were applied to the horizontal members, brace members, and main posts to confirm the effects of horizontal members on the overall behavior of the transmission tower.

Using the commercial analysis software ABAQUS, B31 beam elements with six degrees of freedom were applied to the analytical models. The inclined angle, shape, and orientation of the members were realistically modeled using beam elements. The connection between the members is fastened by multiple bolts. Therefore, some researchers concluded that the multiple-bolts connection can provide rotational constraints [38-39]. Reflecting the connection characteristics, the entire members of the examined transmission towers were modeled with beam elements. In addition, the stress at the predefined reference points at the sections was calculated, therefore the inelasticity of the members and structures could be checked during the nonlinear analysis because the beam sections shown in Fig. 3 were assigned for all the members.

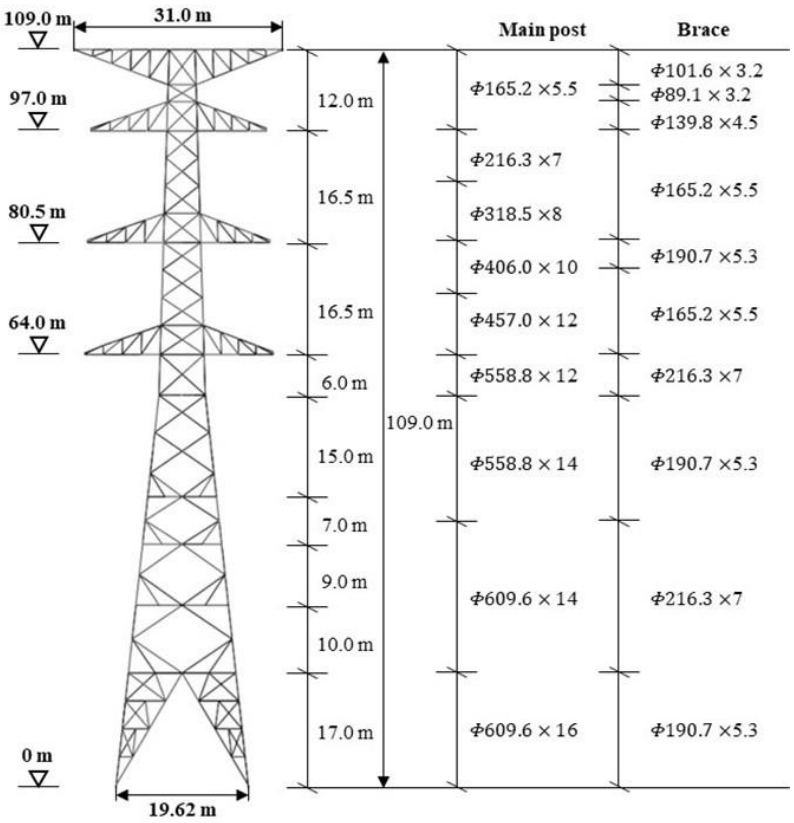

Figure 1. Characteristics and dimensions of the 765 kV-class transmission towers

Preprints (www.preprints.org) | NOT PEER-REVIEWED | Posted: 7 December 2022 doi:10.20944/preprints202212.0129.v1

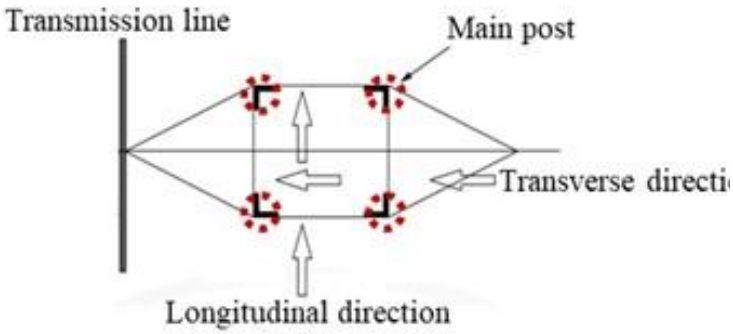

Figure 2. Details of wind directions on a transmission line

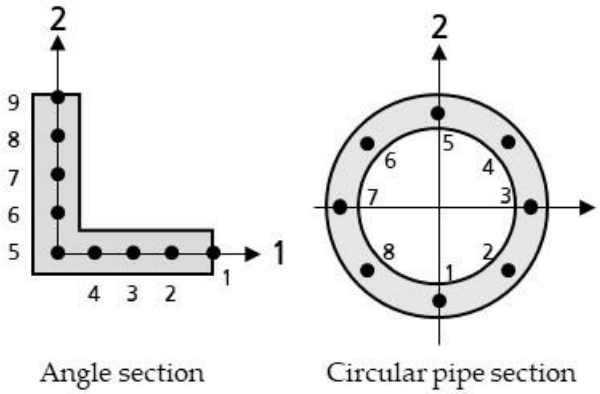

Figure 3. Details of the section members

The load exerted on the ground wires was applied as a concentrated load on the top-most arm. The multi-point constraint (MPC) and reference point were used to exert the load applied in the six arms to support the conductors. The load components were transverse, longitudinal, and vertical loads. The wind load applied to the transmission tower was evenly exerted in a line load throughout the tower. In terms of boundary conditions, the fixed support conditions were applied to the four legs in contact with the ground. Figs. 3 and 4 present the MPC-tie option and the boundary conditions, respectively.

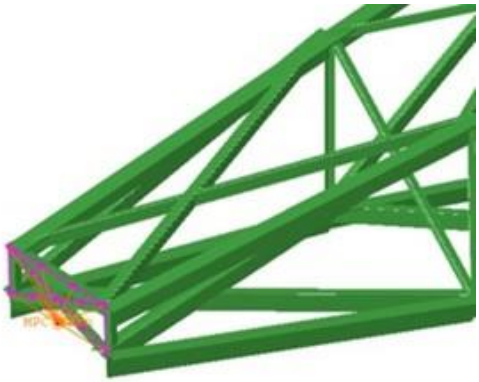

Figure 4. Details of the MPC-tie option

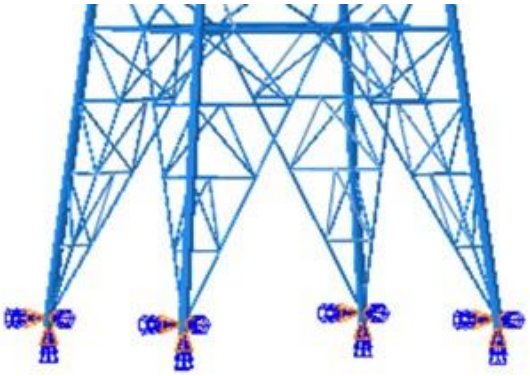

Figure 5. Details of the boundary conditions

Preprints (www.preprints.org) | NOT PEER-REVIEWED | Posted: 7 December 2022 doi:10.20944/preprints202212.0129.v1

Table 1. Section properties of 765-kV transmission tower

Member type	Cross-section (mm×mm)
Main post	Φ609.6×16
	Φ609.6×14
	Φ558.8×14
	Φ558.8×12
	Φ457.0×12
	Φ406.0×10
	Φ318.5×8.0
	Φ216.3×7.0
	Φ165.2×5.5
Brace	Φ216.3×7.0
	Φ190.7×5.3
	Φ165.2×5.5
	Φ139.8×4.5
	Φ101.6×3.2
	Φ89.1×3.2
Horizontal member	Φ216.3×7.0
	Φ190.7×5.3
	Φ165.2×5.5
	Φ139.8×4.5
	Φ89.1×3.2
	Φ76.3×2.8

Table 2. Description of the conductors and ground wires

Parameters	Conductor	Ground wire
Specification	ACSR (cardinal)	AWS-200
Rated tension strength (kN)	150	126
Unit weight (N/m)	17.26	9.42
Outer diameter (m)	0.03	0.018
Area (mm2)	547.3	204.3
Modulus of elasticity (GPa)	74.2	108.8
Thermal expansion coefficient (10-6/℃)	23	15.5

Preprints (www.preprints.org) | NOT PEER-REVIEWED | Posted: 7 December 2022 doi:10.20944/preprints202212.0129.v1

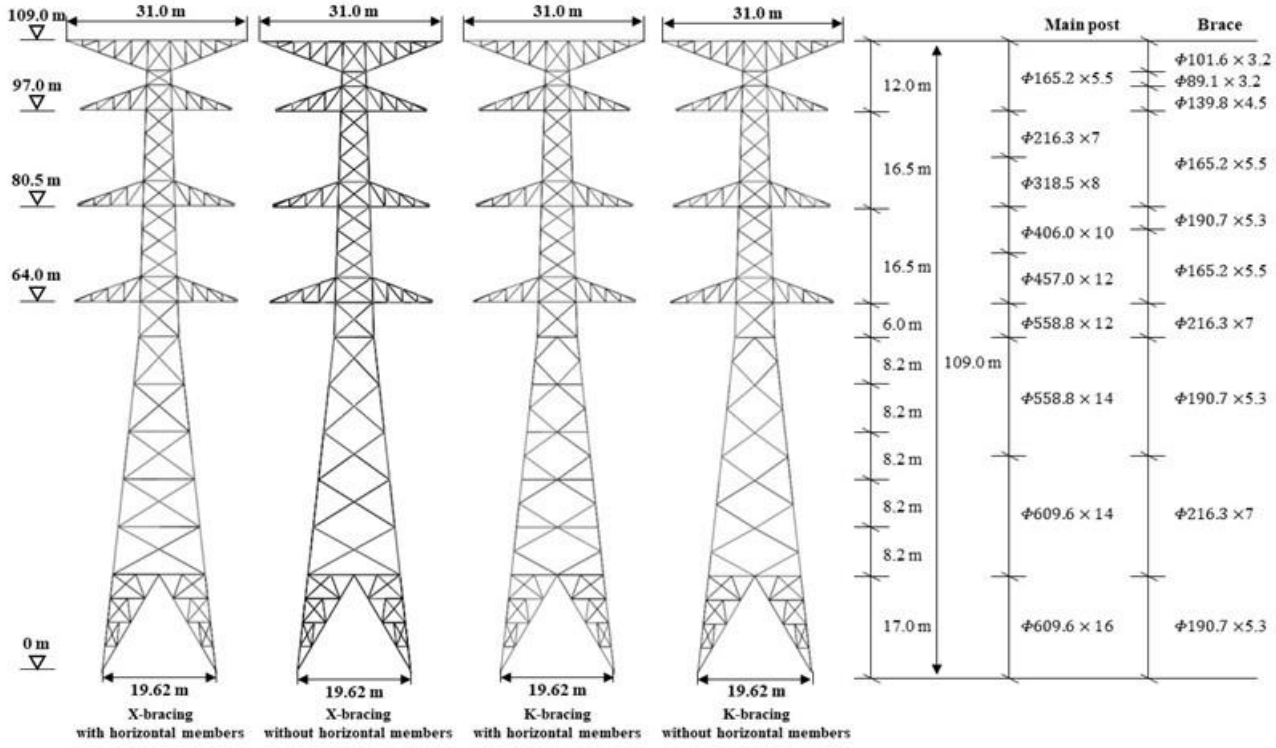

(a)

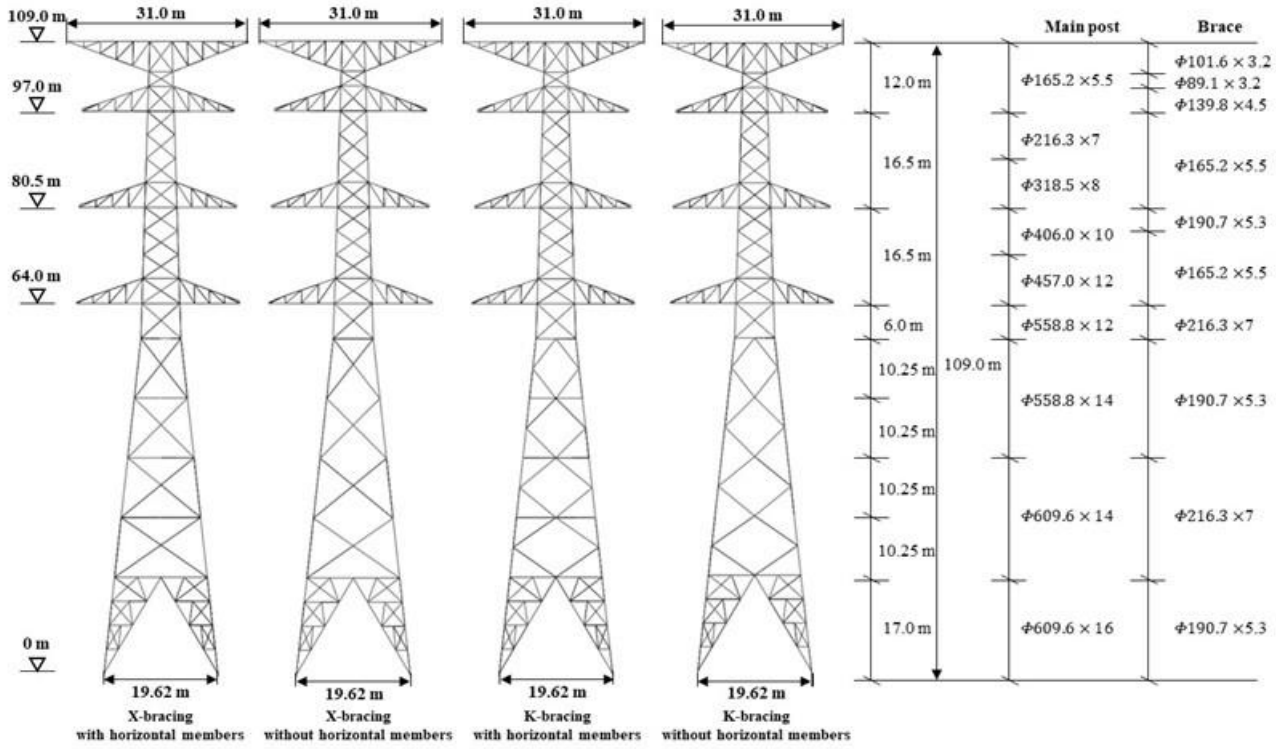

(b)

Preprints (www.preprints.org) | NOT PEER-REVIEWED | Posted: 7 December 2022 doi:10.20944/preprints202212.0129.v1

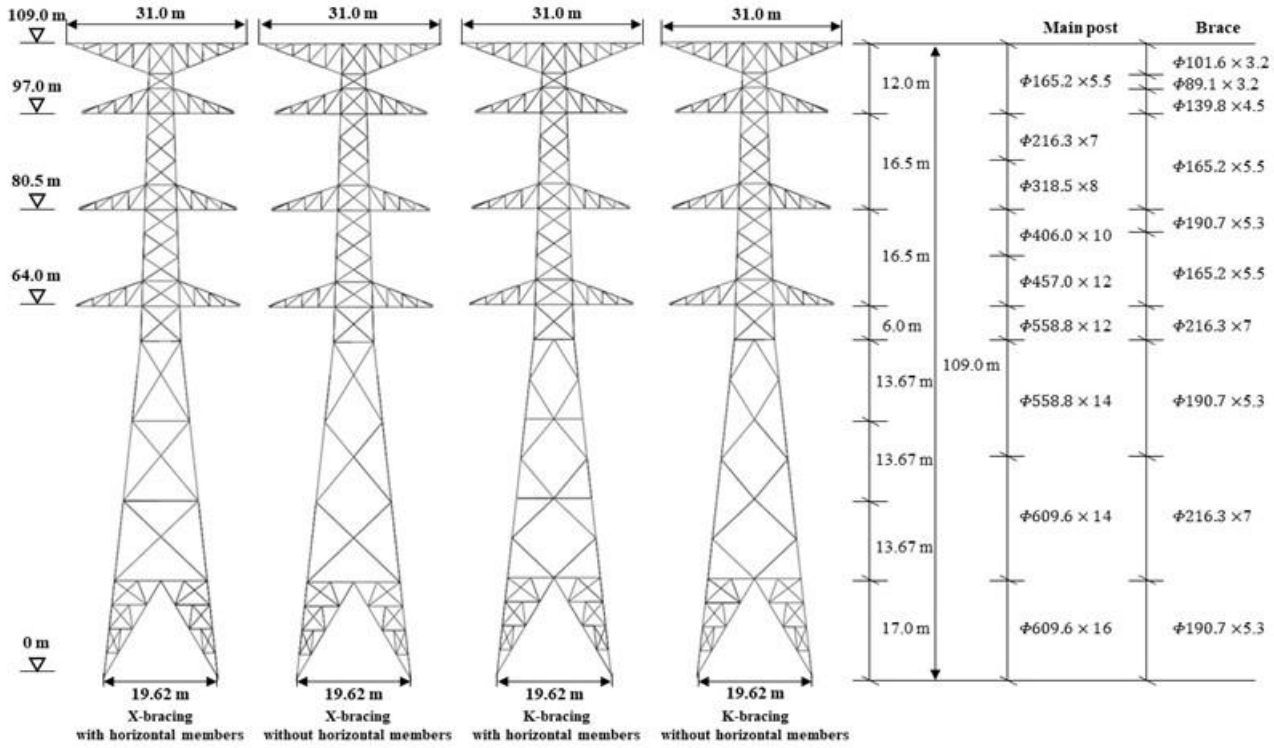

(c)

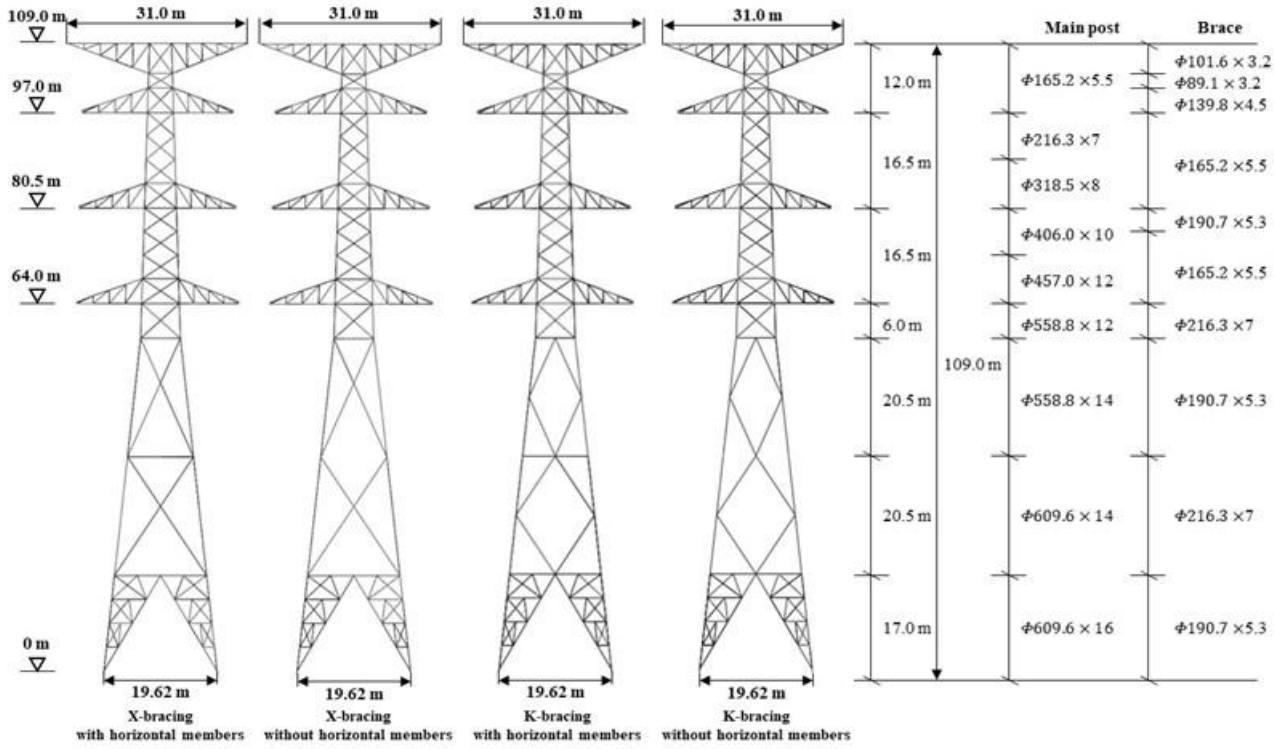

(d)

Figure 6. Description of parametric variables in the analytical models: (a) Models with five equal braces; (b) Models with four equal braces; (c) Models with three equal braces; (d) Models with two equal braces

Preprints (www.preprints.org) | NOT PEER-REVIEWED | Posted: 7 December 2022 doi:10.20944/preprints202212.0129.v1

2.1.2 Parametric variables of the analytical model

Parametric studies were conducted to analyze the effects of horizontal and brace members on improving the load-carrying capacity of the transmission tower. The variables of the research were the presence of horizontal members, shape of braces, and brace spacing. The role of the horizontal member is to prevent distortion and maintain the shape of the structure. To confirm the torsional resistance and distortion of the transmission tower with the effects of the horizontal members, variables indicating the presence of horizontal members were applied in the models. To affect the slenderness ratio of the members, the lengths of the main post and braces were modulated by the equal spacing and shape of the braces. However, the section properties of the brace and the main post were maintained. The shape of a brace can be categorized into two types: X and K bracing. X bracing is a shape in which braces, horizontal members, and main posts are gathered in one place. K bracing is a shape in which bracing exists between horizontal members to support the middle part of the main post. The equal spacing of braces is categorized into four types: five to two equal spacings. The respective spacings of the five, four, three, and two equal spacings were 8.2 m, 10.25 m, 13.67 m, and 20.5 m per spacing. The variables used in the analytical models are shown in Fig. 5; it shows the models with equal spacing of the braces, the differences owing to the shape of the braces, and the presence or absence of horizontal members. Structural analysis was performed on a total of sixteen models. The positions of the horizontal members and the coordinate system of the displacements are shown in Fig. 6. The transverse displacement at the front of the tower, longitudinal displacement at the front of the tower, and vertical displacement were named Ux, Uy, and Uz, respectively. The horizontal member of the lowest part was named Lv1 and of the uppermost part Lv6.

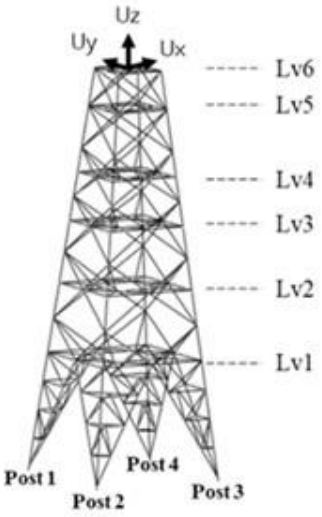

Figure 7. Description of horizontal member position and the coordinate system of displacements

2.1 Analytical load combination and method

2.2.1 Design load and load combination

The wind load and broken wire load conditions are exerted in the lattice transmission tower based on the ASCE74 (Guidelines for Electrical Line Structural Loading, 4th edition) design standard. Linear static, eigenvalue, and geometric nonlinear and inelastic analyses were performed to analyze the effect of the horizontal and brace members on enhancing the load-carrying capacity of the transmission tower. Linear static, eigenvalue, and geometric nonlinear and inelastic analyses were performed to analyze the effect of the horizontal and brace members on structural behavior. The horizontal members and braces maintain the distance between the main post and reduce the effective buckling length. It also serves to prevent twisting of the constituting shape. A linear static analysis was

 doi:10.20944/preprints202212.0129.v1

performed to observe the effect of the horizontal and brace members on the resistance of the torsion and distortion of the tower due to the broken wire loads categorized into three types: longitudinal, transverse, and vertical loads. Eigenvalue analysis was performed to confirm if the effective buckling length was reduced due to the effect of horizontal members and braces, thereby improving the elastic buckling strength. Finally, geometric nonlinear and inelastic analysis was performed to explore the effect of the buckling strength improvement of the secondary members on the load-carrying capacity. Eigenvalue and geometric nonlinear and inelastic analyses were performed by applying the wind load condition to the transmission tower. Table 3 shows the summary of the analysis methodologies and their objectives in this study. Details are described in the next sections.

Table 3. Summary of the analytical investigation

Analysis type	Objective	Applied load case
Linear static analysis	To see the effect on the torsional and distortional resistance	Broken wire case
Eigenvalue analysis	To see the effect on the elastic buckling resistance	Wind load case
Geometric nonlinear and inelastic analysis	To see the effect on the load-carrying capacity	Wind load case

Local conditions, topographical conditions, wind gusts, tower shape, and height must be considered to exert the load used in load combinations. The local conditions of exposure C Are recommended by the ASCE74; thus, the load combination was calculated for exposure C. A panel was set for each height of the tower, and the wind load was applied to the panel. In research, the wind load is considered a common load condition, and the broken wire condition inducing torsional loads is considered an abnormal load condition. The wire loads were applied based on the calculation of the wire tension owing to the states of change. It can be calculated given that the conditions of the initial and final states were known. The wind load based on the ASCE74 was calculated. Kz, Kzt, V100, G, Cf, and A are required to calculate the wind loads. Kz is the wind pressure exposure coefficient, Kzt is the topographic factor, V100 is the reference 3-second wind speed for the 100-year mean recurrence interval (m/s), G is the gust response factor for conductors, ground wires, and structures, Cf is the force coefficient value, and A is the area projected on the plane normal to the wind direction (m2).

2.2.2 Linear static analysis

Linear static analysis was performed to observe the distortion and torsional stiffness of the transmission tower owing to the horizontal and brace members. The role of the horizontal and brace members is to resist distortion and maintain the original shape, support resisting the torsional loads applied in the main post, and reduce the effective buckling length to prevent buckling. Broken wire load conditions inducing torsion were applied to the transmission towers to analyze the effect of the horizontal and brace members on the torsional loads. Broken wire loads are divided into four types: disconnection of the ground wire, 1st-floor conductor, 2nd-floor conductor, and 3rd-floor conductor. The broken load condition of the ground wire was named GW, and the broken load conditions of the 1st-, 2nd-, and 3rd-floor conductors were named CD1, CD2, and CD3, respectively. Descriptions of the four load conditions with broken wires are presented in Fig. 7. V, T, and L are the vertical, lateral, and longitudinal loads, respectively.

Preprints (www.preprints.org) | NOT PEER-REVIEWED | Posted: 7 December 2022 doi:10.20944/preprints202212.0129.v1

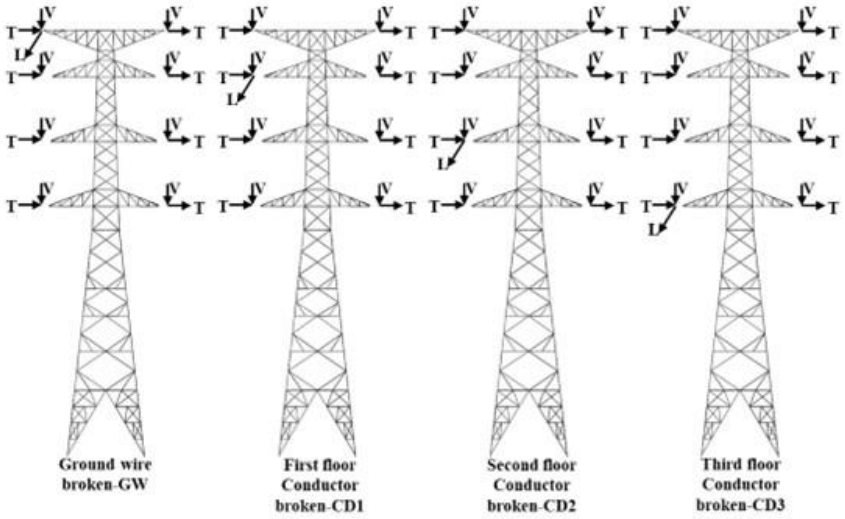

Figure 8. Descriptions of the load conditions with broken wires

2.2.3 Eigenvalue analysis

The elastic buckling strength and eigenmode of an ideal structure can be predicted using an eigenvalue analysis. The eigenmode can predict the buckling mode based on geometric characteristics. It was necessary to confirm that the transmission tower had sufficient elastic buckling strength. The Lanczos eigensolver was used as the method. Eigenvalue analysis was performed by avoiding overlapping of the eigenvalues and eigenmodes. Models with various variables were analyzed to identify the factors affecting the elastic buckling strength of the transmission tower, and the effects of the presence of horizontal members and the spacing and shape of the braces on the elastic buckling strength were studied under 0º wind load (transverse direction) conditions

2.2.4 Geometric nonlinear and inelastic analysis

Geometric nonlinear and inelastic analysis of the models with or without horizontal members and models with different shapes and spacings of the braces was performed to analyze the ultimate behavior, weak members, and load-carrying capacity of the transmission tower under 0º wind load (transverse direction) conditions. To consider the material features of the section, the yield strengths of the circular pipe section and angle section were 345 and 290 MPa, respectively, for applying of a bilinear elastic-plastic model. The load conditions were the same as those used in the eigenvalue analysis. The arc length method was used for the geometric nonlinear and inelastic analysis. By analyzing the load-displacement curves in the models with various parameters, the load-carrying capacity of the transmission tower owing to the effect of the horizontal and brace members was confirmed.

3. Contribution of the secondary members to structural behavior and load-carrying capacity

3.1 Comparative studies of linear static behavior

By analyzing the parametric models owing to the horizontal members and the shape of the braces, the brace spacing, displacement of the horizontal position, and distortion of the section shape were determined. To confirm the effect of the secondary members on the torsional load, broken condition loads were applied to the models. Among the load conditions caused by the broken wires, CD1 is the governing load. Therefore, the CD1 load condition was applied to the transmission tower to confirm the displacement and distortion. The transverse, longitudinal, vertical, and torsional displacements were checked at four points at the position where horizontal members and the main post met. The displacements of the equal-spacing brace model under the effect of the secondary members are presented in Tables 4–7; they show the transverse, longitudinal, vertical, and

Preprints (www.preprints.org) | NOT PEER-REVIEWED | Posted: 7 December 2022 doi:10.20944/preprints202212.0129.v1

torsional displacements Ux, Uy, Uz, and UΘ, respectively. In addition, the horizontal member of the lowest part was named Lv1, and the uppermost part was named Lv6. Figs. 8 and 9 show the deformed shapes of the transmission towers under the examined load combinations, obtained by the linear elastic analysis.

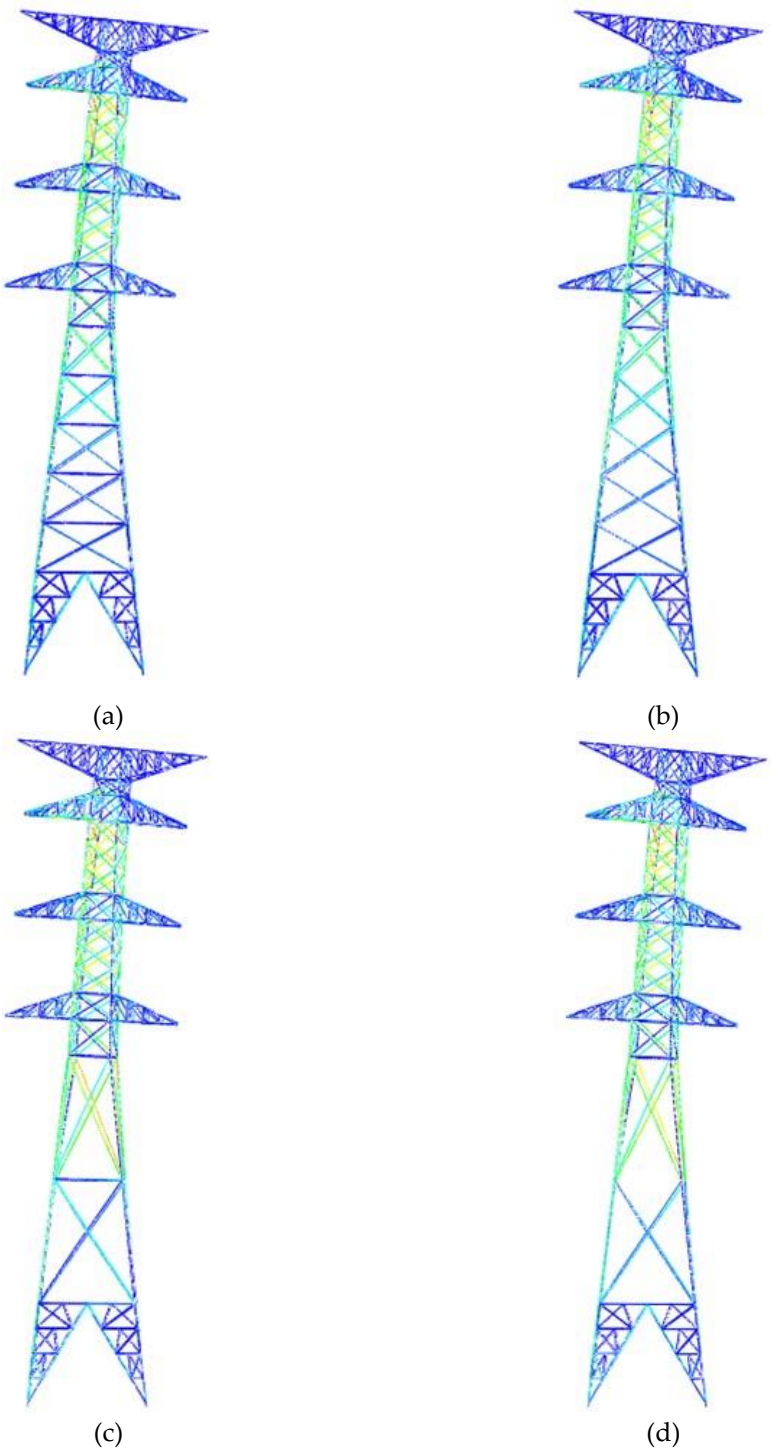

Figure 9. Comparison of the deformed shapes of the transmission towers with X bracing under the considered load combination: (a) Models with five equal spacings and horizontal members; (b) Models with five equal spacings without horizontal members; (c) Models with two equal spacings and horizontal members; (d) Models with two equal spacings without horizontal members

Preprints (www.preprints.org) | NOT PEER-REVIEWED | Posted: 7 December 2022 doi:10.20944/preprints202212.0129.v1

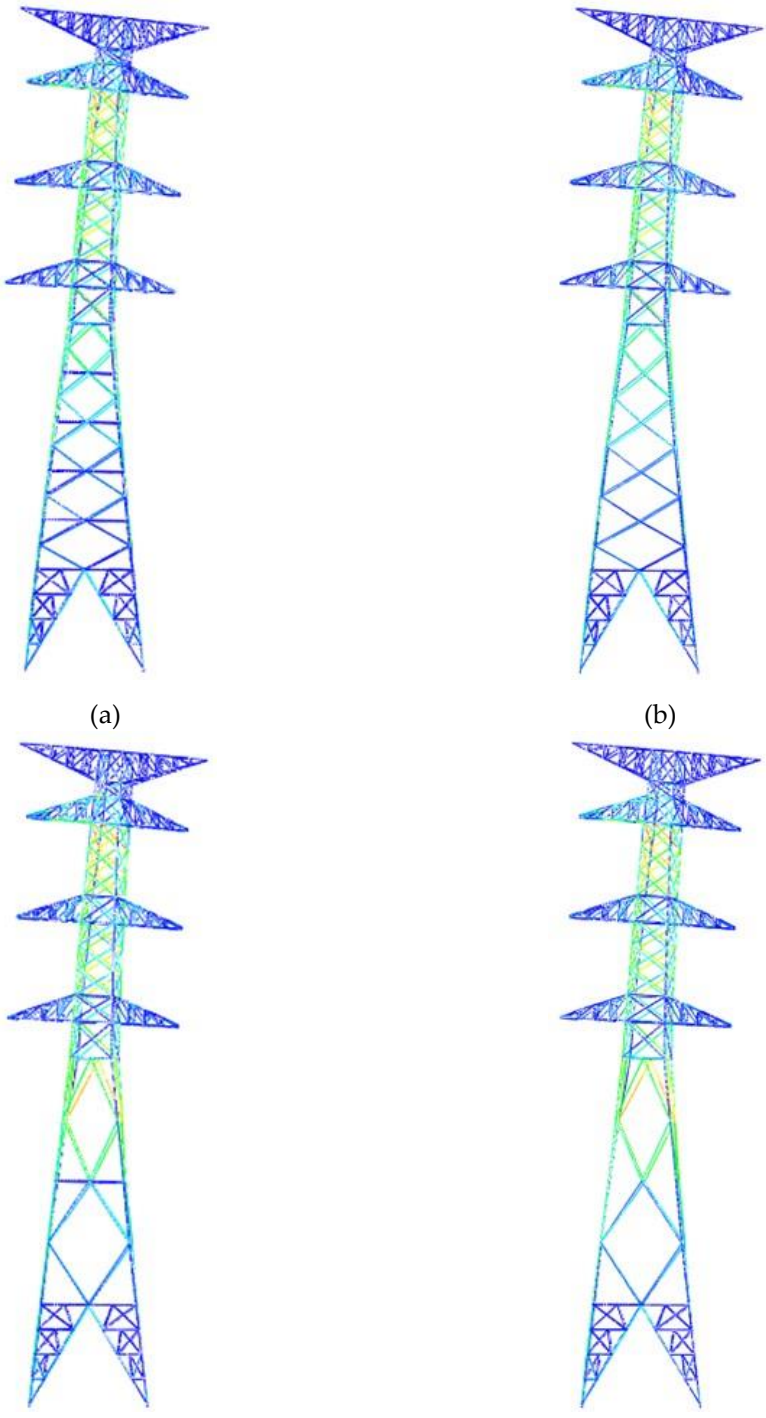

(a) (b)

(c) (d)

Figure 10. Comparison of the deformed shapes of the transmission towers with K bracing under the considered load combination: (a) Models with five equal spacings and horizontal members; (b) Models with five equal spacings without horizontal members; (c) Models with two equal spacings and horizontal members; (d) Models with two equal spacings without horizontal members

Preprints (www.preprints.org) | NOT PEER-REVIEWED | Posted: 7 December 2022 doi:10.20944/preprints202212.0129.v1

Table 4. Brace spacing effect on the displacement of X-bracing models with horizontal members

Spacing		X-brace															
		Post1				Post2				Post3				Post4			
		Ux (mm)	Uy (mm)	Uz (mm)	Uθ (rad)	Ux (mm)	Uy (mm)	Uz (mm)	Uθ (rad)	Ux (mm)	Uy (mm)	Uz (mm)	Uθ (rad)	Ux (mm)	Uy (mm)	Uz (mm)	Uθ (rad)
Five	Lv1	8.8	6.3	0.4	0.001	-3.4	6.6	4.5	0.001	-3.6	-6.1	0.8	0.001	9.0	-5.8	4.9	0.001
	Lv2	13.5	9.6	0.6	0.002	-0.2	10.2	6.6	0.001	-0.6	-4.5	1.2	0.000	14.0	-3.9	7.2	0.001
	Lv3	20.3	14.5	0.7	0.003	5.0	15.1	8.4	0.002	4.5	-1.3	1.5	0.001	20.8	-0.6	9.2	0.002
	Lv4	29.8	21.5	0.7	0.005	12.1	22.1	9.8	0.003	11.6	3.2	1.8	0.002	30.4	3.9	10.8	0.004
	Lv5	43.0	31.3	0.5	0.009	21.3	31.9	10.8	0.006	20.8	9.1	1.8	0.004	43.6	9.8	12.0	0.007
	Lv6	60.1	44.4	0.07	0.015	33.2	44.5	11.1	0.011	33.2	17.8	1.7	0.008	60.2	17.9	12.5	0.013
Four	Lv1	8.7	6.2	0.4	0.001	-3.3	6.6	4.5	0.001	-3.6	-6.2	0.8	0.001	9.1	-5.7	4.9	0.001
	Lv2	14.8	10.5	0.6	0.002	1.0	11.3	7.1	0.001	0.4	-3.9	1.3	0.000	15.5	-3.1	7.7	0.002
	Lv3	24.2	17.3	0.7	0.004	8.4	18.2	9.0	0.002	7.7	0.7	1.7	0.001	25.0	1.7	9.9	0.003
	Lv4	39.5	28.6	0.5	0.008	18.2	29.4	10.5	0.005	17.5	6.7	1.8	0.003	40.3	7.6	11.7	0.006
	Lv5	61.1	45.1	0.02	0.016	31.8	45.2	11.0	0.011	31.7	16.1	1.7	0.007	61.2	16.2	12.4	0.013
Three	Lv1	8.6	6.1	0.4	0.001	-3.3	6.7	4.5	0.001	-3.7	-6.3	0.8	0.001	9.1	-5.6	4.9	0.001
	Lv2	17.6	12.5	0.7	0.002	2.9	13.5	7.7	0.002	2.1	-3.1	1.4	0.000	18.4	-1.9	8.4	0.002
	Lv3	34.2	24.6	0.6	0.006	13.7	25.7	10.0	0.004	12.9	3.3	1.7	0.002	35.1	4.4	11.0	0.005
	Lv4	63.7	47.0	0.09	0.016	28.6	47.1	10.9	0.011	28.5	12.1	1.5	0.006	63.9	12.3	12.2	0.013
Two	Lv1	8.6	6.1	0.4	0.001	-3.2	6.7	4.5	0.001	-3.7	-6.3	0.8	0.001	9.2	-5.5	4.9	0.001
	Lv2	25.6	18.3	0.6	0.004	6.1	19.7	8.7	0.003	5.0	-2.5	1.5	0.001	26.9	-0.9	9.6	0.003
	Lv3	73.2	53.8	0.46	0.019	19.2	54.0	10.7	0.012	19.1	0.2	1.1	0.004	73.4	0.3	11.9	0.015

Table 5. Brace spacing effect on the displacement of X-bracing models without horizontal members

Spacing		X-brace															
		Post1				Post2				Post3				Post4			
		Ux (mm)	Uy (mm)	Uz (mm)	Uθ (rad)	Ux (mm)	Uy (mm)	Uz (mm)	Uθ (rad)	Ux (mm)	Uy (mm)	Uz (mm)	Uθ (rad)	Ux (mm)	Uy (mm)	Uz (mm)	Uθ (rad)
Five	Lv1	8.9	6.4	0.4	0.001	-3.4	6.5	4.5	0.001	-3.5	-6.0	0.8	0.001	9.0	-5.9	4.9	0.001
	Lv2	13.2	9.2	0.6	0.002	0.1	10.6	6.6	0.001	-0.9	-5.0	1.2	0.001	14.4	-3.4	7.2	0.001
	Lv3	20.2	14.3	0.7	0.003	5.1	15.2	8.4	0.002	4.4	-1.4	1.6	0.001	21.1	-0.4	9.2	0.002
	Lv4	29.8	21.2	0.7	0.005	12.2	22.4	9.8	0.003	11.4	3.1	1.8	0.002	30.8	4.4	10.9	0.004
	Lv5	42.4	30.5	0.5	0.009	22.1	32.8	10.8	0.006	20.2	8.4	1.9	0.004	44.8	11.0	12.0	0.008
	Lv6	60.6	44.8	0.05	0.016	33.5	44.8	11.3	0.012	33.6	18.2	1.8	0.008	60.6	18.1	12.7	0.013
Four	Lv1	8.9	6.4	0.4	0.001	-3.4	6.5	4.5	0.001	-3.5	-5.9	0.8	0.001	9.0	-5.9	4.9	0.001
	Lv2	14.2	9.7	0.6	0.002	1.6	12.1	7.0	0.001	-0.2	-4.9	1.3	0.001	16.3	-2.0	7.6	0.002
	Lv3	24.4	17.4	0.7	0.004	8.4	18.2	9.2	0.002	7.8	0.9	1.7	0.001	25.2	1.9	10.1	0.003
	Lv4	38.4	27.3	0.5	0.007	19.7	31.1	10.5	0.006	16.6	5.3	1.8	0.003	42.2	9.6	11.6	0.007
	Lv5	61.8	45.7	0.01	0.016	32.4	45.7	11.3	0.012	32.4	16.7	1.7	0.008	61.9	16.6	12.7	0.013
Three	Lv1	8.8	6.3	0.4	0.001	-3.4	6.5	4.5	0.001	-3.6	-6.0	0.8	0.001	9.0	-5.8	4.9	0.001
	Lv2	16.6	11.2	0.6	0.002	3.8	14.8	7.6	0.002	1.3	-4.4	1.4	0.001	19.6	-0.3	8.3	0.002
	Lv3	32.8	23.1	0.6	0.006	15.6	27.7	10.0	0.005	11.7	1.6	1.8	0.002	37.5	6.9	11.0	0.005
	Lv4	64.9	47.9	0.1	0.017	29.7	48.0	11.2	0.012	29.7	13.1	1.6	0.007	65.0	13.1	12.6	0.014
Two	Lv1	8.9	6.4	0.4	0.001	-3.4	6.4	4.6	0.001	-3.4	-5.8	0.8	0.001	8.9	-5.9	4.9	0.001
	Lv2	21.4	13.4	0.6	0.003	10.6	25.4	8.3	0.003	1.5	-8.1	1.4	0.001	32.3	5.7	9.0	0.004
	Lv3	75.3	55.5	0.46	0.019	21.1	55.6	11.2	0.012	21.2	1.8	1.3	0.004	75.4	1.8	12.6	0.016

Table 6 Brace spacing effect on the displacement of K-bracing models with horizontal members

Preprints (www.preprints.org) | NOT PEER-REVIEWED | Posted: 7 December 2022 doi:10.20944/preprints202212.0129.v1

Spacing		X-brace															
		Post1				Post2				Post3				Post4			
		Ux (mm)	Uy (mm)	Uz (mm)	Uθ (rad)	Ux (mm)	Uy (mm)	Uz (mm)	Uθ (rad)	Ux (mm)	Uy (mm)	Uz (mm)	Uθ (rad)	Ux (mm)	Uy (mm)	Uz (mm)	Uθ (rad)
Five	Lv1	8.3	5.9	0.4	0.001	-3.0	6.1	4.5	0.001	-3.1	-5.5	0.8	0.001	8.5	-5.3	4.8	0.001
	Lv2	13.2	9.4	0.6	0.002	0.1	9.7	6.6	0.001	-0.1	-3.9	1.2	0.000	13.4	-3.6	7.2	0.001
	Lv3	20.0	14.4	0.7	0.003	5.2	14.6	8.4	0.002	5.0	-0.7	1.6	0.001	20.3	-0.4	9.2	0.002
	Lv4	29.7	21.4	0.7	0.005	12.2	21.8	9.8	0.003	11.9	3.6	1.8	0.002	30.0	4.0	10.9	0.004
	Lv5	43.0	31.4	0.5	0.009	21.5	31.6	10.8	0.006	21.3	9.6	1.9	0.004	43.3	9.9	12.1	0.007
	Lv6	61.1	45.1	0.02	0.016	32.8	44.9	11.2	0.011	33.0	17.3	1.7	0.008	61.1	17.1	12.6	0.013
Four	Lv1	8.3	5.9	0.4	0.001	-3.0	6.1	4.5	0.001	-3.1	-5.5	0.8	0.001	8.5	-5.3	4.8	0.001
	Lv2	14.6	10.5	0.6	0.002	1.2	10.7	7.1	0.001	1.0	-3.2	1.3	0.000	14.9	-2.9	7.8	0.002
	Lv3	24.3	17.4	0.7	0.004	8.5	17.7	9.1	0.002	8.3	1.4	1.7	0.001	24.5	1.8	10.0	0.003
	Lv4	39.7	28.8	0.5	0.008	18.5	29.1	10.6	0.005	18.3	7.4	1.8	0.003	39.9	7.7	11.8	0.006
	Lv5	62.4	46.0	0.04	0.016	31.7	45.8	11.2	0.011	31.9	15.9	1.7	0.007	62.3	15.6	12.6	0.013
Three	Lv1	8.3	5.9	0.4	0.001	-3.0	6.1	4.5	0.001	-3.1	-5.5	0.8	0.001	8.4	-5.3	4.8	0.001
	Lv2	17.6	12.6	0.7	0.002	3.0	12.8	7.9	0.001	2.8	-2.2	1.5	0.000	17.8	-1.9	8.6	0.002
	Lv3	35.0	25.3	0.6	0.006	13.8	25.5	10.2	0.004	13.6	3.9	1.8	0.002	35.2	4.1	11.3	0.005
	Lv4	66.1	48.5	0.2	0.017	28.8	48.4	11.2	0.012	28.9	11.8	1.6	0.006	66.0	11.6	12.6	0.014
Two	Lv1	8.3	5.9	0.4	0.001	-2.9	6.1	4.5	0.001	-3.1	-5.4	0.8	0.001	8.4	-5.2	4.9	0.001
	Lv2	26.5	19.0	0.6	0.004	6.5	19.2	9.2	0.003	6.3	-1.2	1.6	0.001	26.7	-1.0	10.1	0.003
	Lv3	77.4	56.4	0.6	0.020	20.5	56.3	11.3	0.012	20.6	0.1	1.2	0.004	77.3	-0.1	12.6	0.016

Table 7 Brace spacing effect on the displacement of K-bracing models without horizontal members

Spacing		X-brace															
		Post1				Post2				Post3				Post4			
		Ux (mm)	Uy (mm)	Uz (mm)	Uθ (rad)	Ux (mm)	Uy (mm)	Uz (mm)	Uθ (rad)	Ux (mm)	Uy (mm)	Uz (mm)	Uθ (rad)	Ux (mm)	Uy (mm)	Uz (mm)	Uθ (rad)
Five	Lv1	8.3	5.9	0.4	0.001	-3.0	6.1	4.5	0.001	-3.1	-5.5	0.8	0.001	8.4	-5.3	4.9	0.001
	Lv2	12.8	8.9	0.6	0.002	0.8	10.5	6.5	0.001	-0.4	-4.5	1.2	0.000	14.2	-2.6	7.1	0.001
	Lv3	20.0	14.2	0.7	0.003	5.6	14.8	8.4	0.002	5.1	-0.5	1.6	0.001	20.5	0.1	9.2	0.002
	Lv4	29.3	20.8	0.7	0.005	13.0	22.5	9.7	0.004	11.7	3.2	1.8	0.002	30.8	5.1	10.7	0.004
	Lv5	42.5	30.8	0.5	0.009	22.7	32.4	10.7	0.006	21.3	9.6	1.9	0.004	44.2	11.4	11.9	0.007
	Lv6	61.4	45.3	0.01	0.016	33.0	45.1	11.3	0.012	33.1	17.5	1.8	0.008	61.3	17.2	12.7	0.013
Four	Lv1	8.3	5.9	0.4	0.001	-3.0	6.1	4.5	0.001	-3.1	-5.5	0.8	0.001	8.4	-5.3	4.9	0.001
	Lv2	14.1	9.7	0.6	0.002	2.3	11.9	6.9	0.001	0.8	-3.9	1.3	0.000	16.0	-1.4	7.5	0.002
	Lv3	24.4	17.3	0.7	0.004	9.1	18.6	9.0	0.003	8.0	1.0	1.7	0.001	25.6	2.5	9.9	0.003
	Lv4	38.6	27.7	0.5	0.007	20.7	30.6	10.3	0.006	18.3	7.1	1.8	0.003	41.5	10.5	11.5	0.007
	Lv5	62.8	46.2	0.04	0.016	31.9	46.0	11.3	0.012	32.1	16.0	1.7	0.007	62.6	15.8	12.7	0.013
Three	Lv1	8.3	6.0	0.4	0.001	-3.0	6.1	4.5	0.001	-3.1	-5.4	0.8	0.001	8.4	-5.3	4.9	0.001
	Lv2	16.6	11.1	0.6	0.002	5.2	15.2	7.4	0.002	2.3	-3.6	1.4	0.000	20.1	1.0	8.1	0.002
	Lv3	33.3	23.6	0.6	0.006	17.1	27.4	9.8	0.005	14.0	3.8	1.7	0.002	37.0	8.2	10.8	0.005
	Lv4	66.4	48.7	0.19	0.017	28.9	48.6	11.3	0.012	29.1	11.9	1.6	0.006	66.3	11.7	12.7	0.014
Two	Lv1	8.3	6.0	0.4	0.001	-3.0	6.1	4.5	0.001	-3.1	-5.4	0.8	0.001	8.4	-5.3	4.9	0.001
	Lv2	23.2	14.9	0.5	0.003	14.3	25.9	7.7	0.004	5.9	-3.9	1.4	0.001	33.0	8.8	8.4	0.004
	Lv3	77.8	56.7	0.6	0.020	20.7	56.5	11.4	0.012	20.9	0.3	1.2	0.004	77.7	0.0	12.8	0.016

Preprints (www.preprints.org) | NOT PEER-REVIEWED | Posted: 7 December 2022 doi:10.20944/preprints202212.0129.v1

Horizontal members and braces rarely affected the displacement up to the model with three equal spacings. There was an effect on the displacement according to the shape of the brace in the model with two equal spacings in which the slenderness ratio was increased, and the effect of the horizontal member is negligible. In addition, the secondary members did not affect the torsional displacement in any of the models.

By applying a displacement to the position of horizontal members, the extent of distortion contributed to by the presence of the horizontal members was determined. Fig. 10 showed the extent of distortion of models with X bracing, and Fig. 11 showed the extent of distortion of models with K bracing. The shape of the structure was shown as a rectangle, according to the position of the horizontal member. Although there was a slight movement in the position of the horizontal member at the top point, it maintained a rectangular shape. Therefore, there were no effects on distortion caused by the presence or absence of horizontal members.

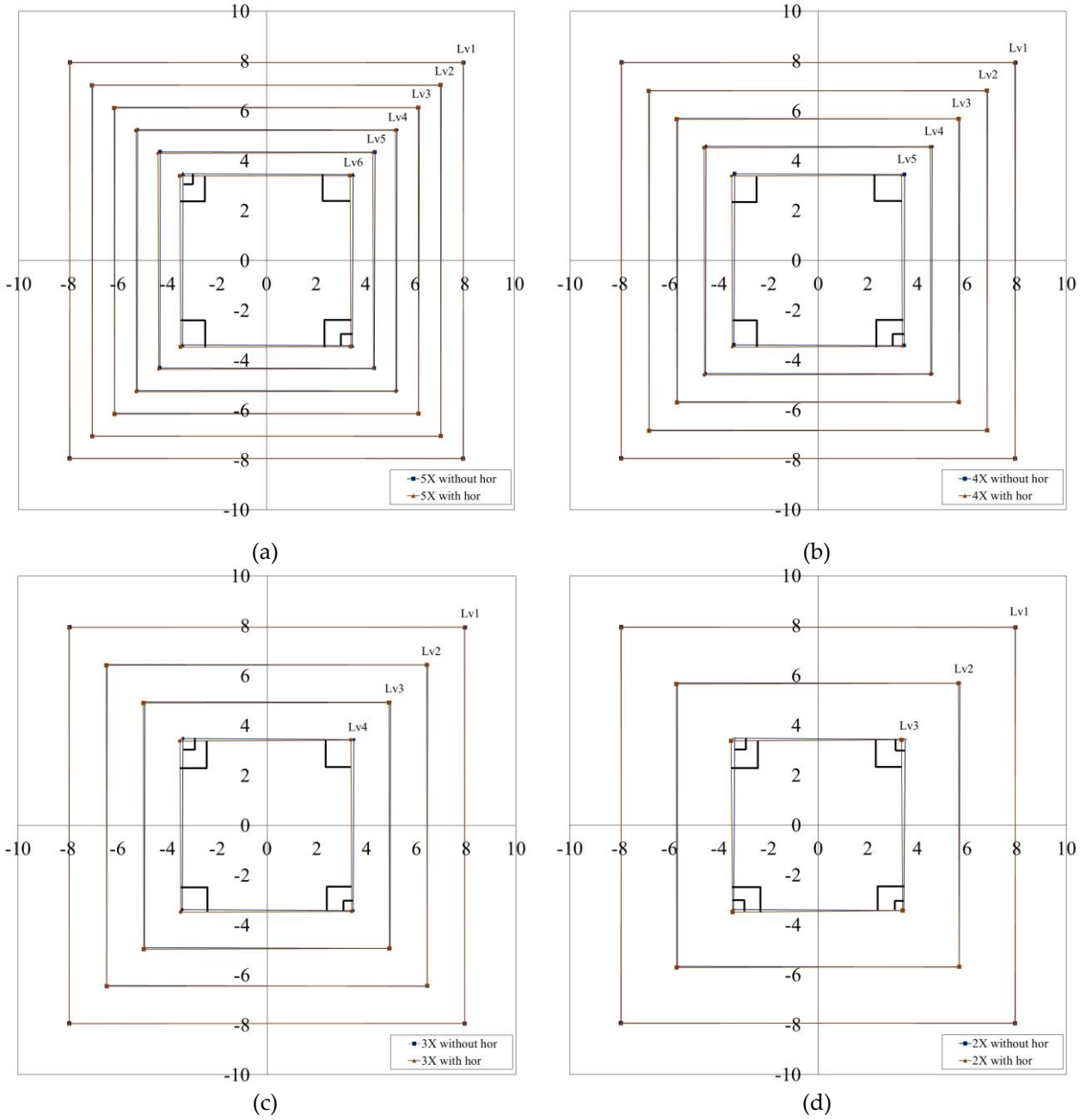

Figure 11. Comparison of the distortion effect of the presence or absence of horizontal members in the models with X bracing: (a) Models with five equal spacings; (b) Models with four equal spacings; (c) Models with three equal spacings; (d) Models with two equal spacings

Preprints (www.preprints.org) | NOT PEER-REVIEWED | Posted: 7 December 2022 doi:10.20944/preprints202212.0129.v1

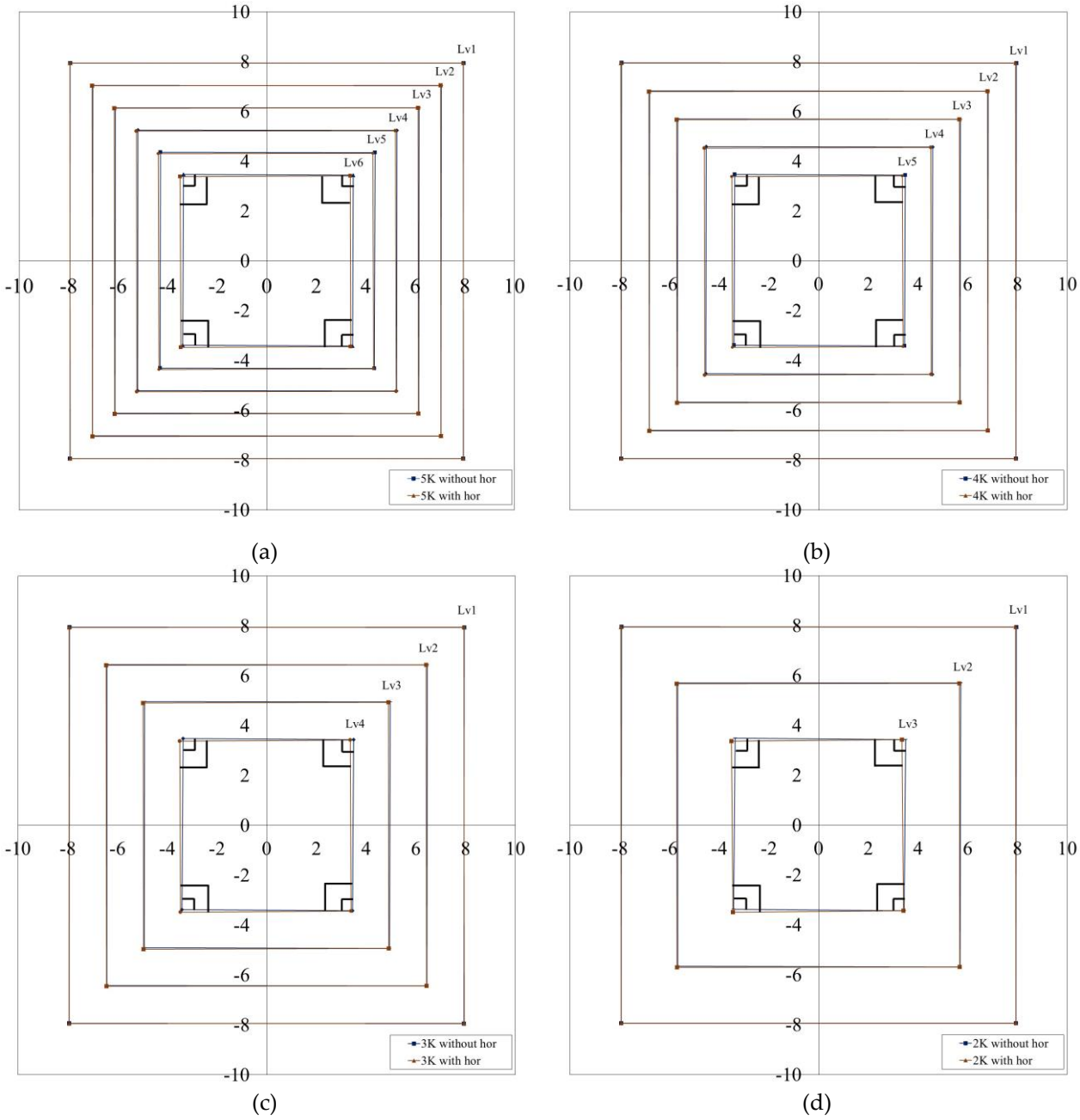

Figure 12. Comparison of the distortion effect of the presence or absence of horizontal members in the models with K bracing: (a) Models with five equal spacings; (b) Models with four equal spacings; (c) Models with three equal spacings; (d) Models with two equal spacings

3.2 Comparative studies of eigenvalues and corresponding modes

By changing the shape of the brace and the spacing between the braces, the effect of the presence of horizontal members was confirmed by the eigenvalues and eigenmodes. Figs. 12 and 13 show the eigenvalues and corresponding eigenmode shapes of the numerical models under the examined load combination. As shown in the figures, bracing and horizontal members can be buckled as well as the main posts at each elastic buckling mode. Although the buckling mode occurred in some members such as cross-arms and braces locally, in this study, global buckling was defined as buckling that occurs simultaneously in the main post and braces of the body part.

Preprints (www.preprints.org) | NOT PEER-REVIEWED | Posted: 7 December 2022 doi:10.20944/preprints202212.0129.v1

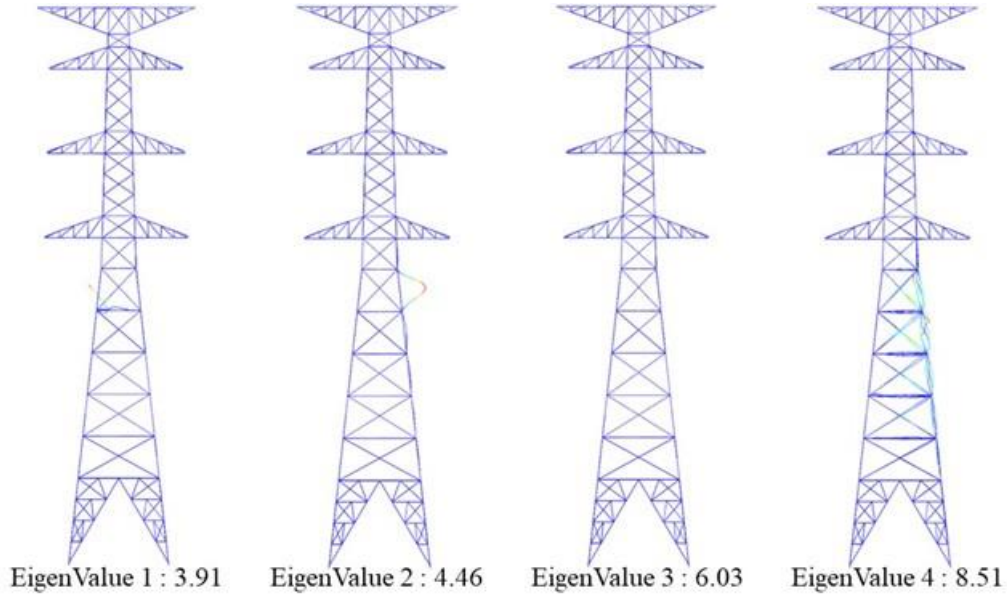

(a)

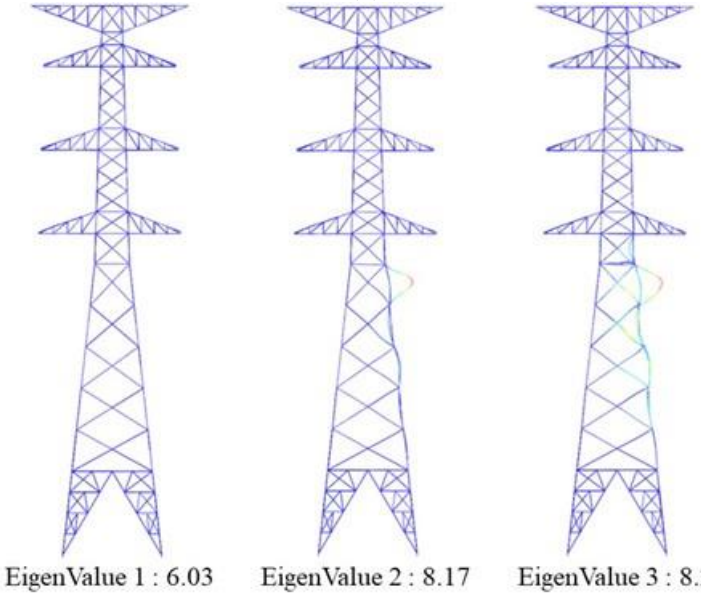

(b)

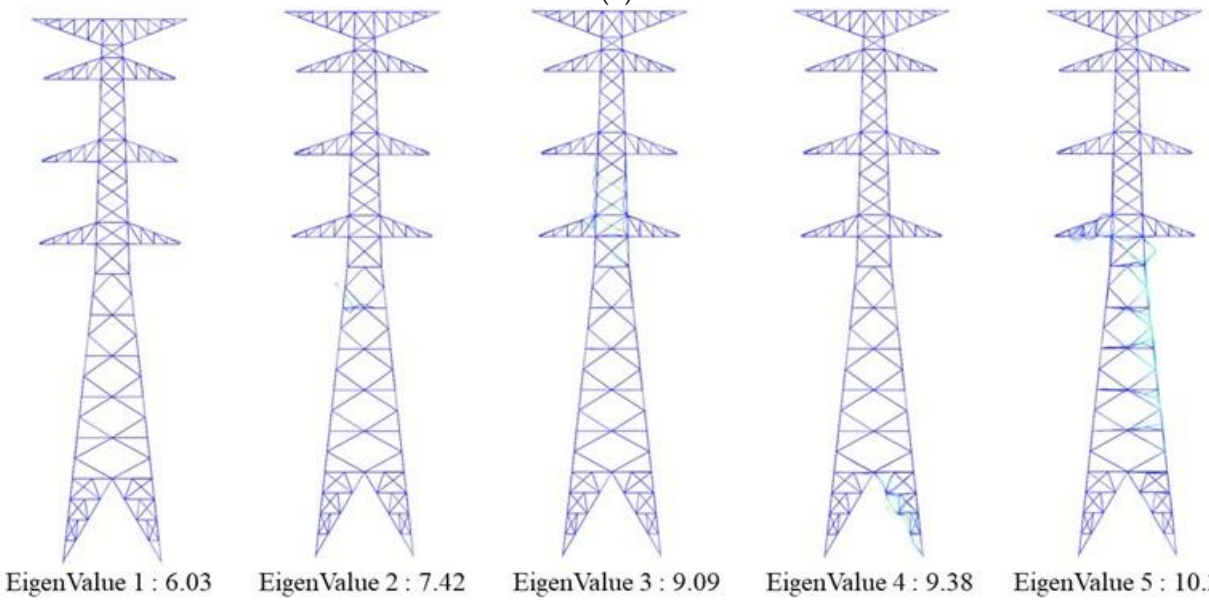

Preprints (www.preprints.org) | NOT PEER-REVIEWED | Posted: 7 December 2022 doi:10.20944/preprints202212.0129.v1

(c)

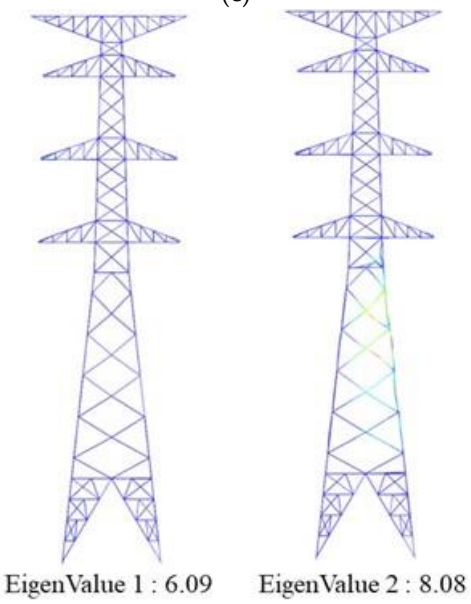

(d)

Figure 13. Changes in eigenvalue and corresponding mode shape of the transmission tower models with five equal braces: (a) Model with X braces and horizontal members; (b) Model with X braces without horizontal members; (c) Model with K braces and horizontal members; (d) Model with K braces without horizontal members

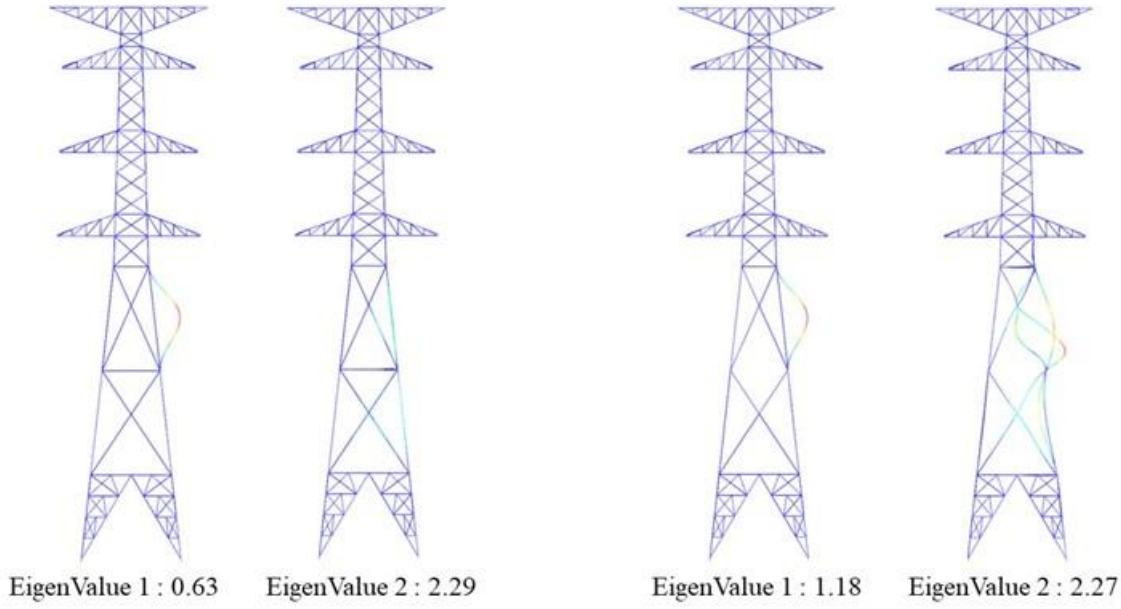

(a) (b)

Preprints (www.preprints.org) | NOT PEER-REVIEWED | Posted: 7 December 2022 doi:10.20944/preprints202212.0129.v1

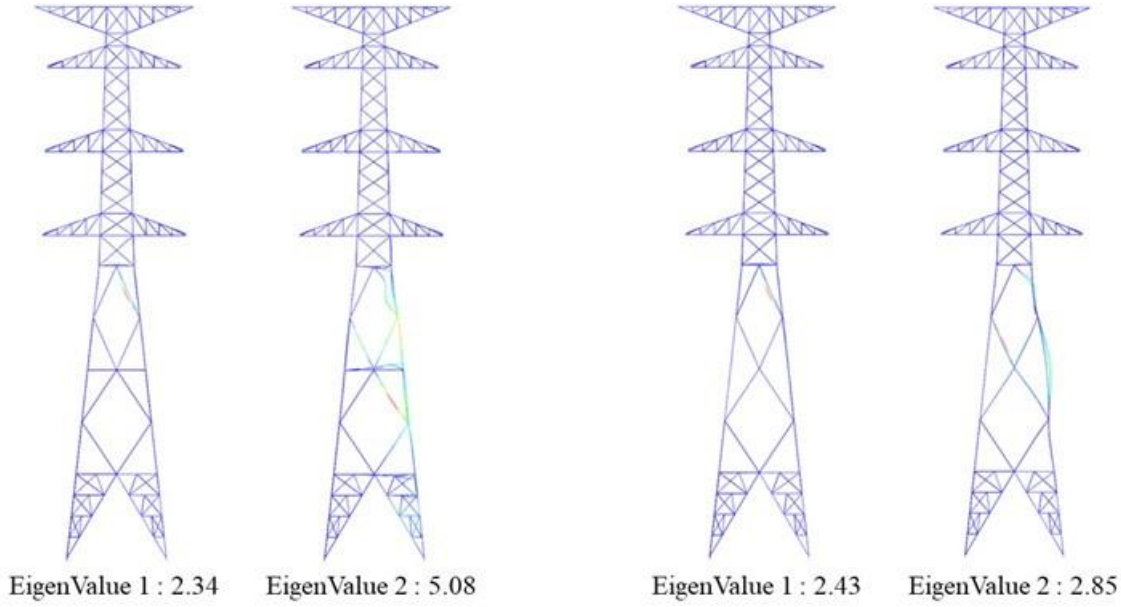

Figure 14. Changes in eigenvalue and corresponding mode shape of the transmission tower models with five equal braces: (a) Model with X braces and horizontal members; (b) Model with X braces without horizontal members; (c) Model with K braces and horizontal members; (d) Model with K braces without horizontal members

The difference in the elastic buckling strength based on the effect of the horizontal members and braces was shown in Fig. 14 and the elastic buckling strength was confirmed in the global buckling mode shape in which buckling occurred at the same time in the main post and brace members. Because the elastic buckling strength was affected by the slenderness ratio, the slenderness ratio criteria of the ASCE 10-15 specification were confirmed. ASCE 10-15 mentions that the slenderness ratio of the main post should be 200 or more, and the brace members should be 250 or more. Accordingly, the slenderness ratio of a model with two equal spacings with the highest slenderness ratio was 74.2 and satisfied the ASCE 10-15 specification. The elastic buckling strength decreased as the spacing of the braces increased, and the difference owing to the shape of the braces and the presence or absence of horizontal members was confirmed. Models with five and two equal spacings were determined as representative models to show the eigenvalues and eigenmodes of the effects of different equal spacings. Figs. 15 and 16 showed the eigenvalues and eigenmodes in the models with five and two equal bracings affected by the horizontal members and the bracing shape. The elastic buckling strength of the model with X bracing was less affected by the presence of the horizontal members than K bracing. As the slenderness ratio increased, the effect of the horizontal members was maximized. The horizontal member reduced the effective buckling length to effectively enhance the elastic buckling strength in K bracing.

Preprints (www.preprints.org) | NOT PEER-REVIEWED | Posted: 7 December 2022 doi:10.20944/preprints202212.0129.v1

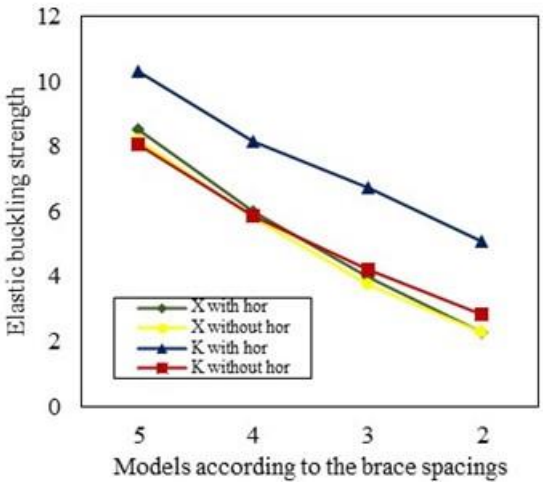

Figure 15. Comparison of elastic buckling strength based on the effect of braces and horizontal members

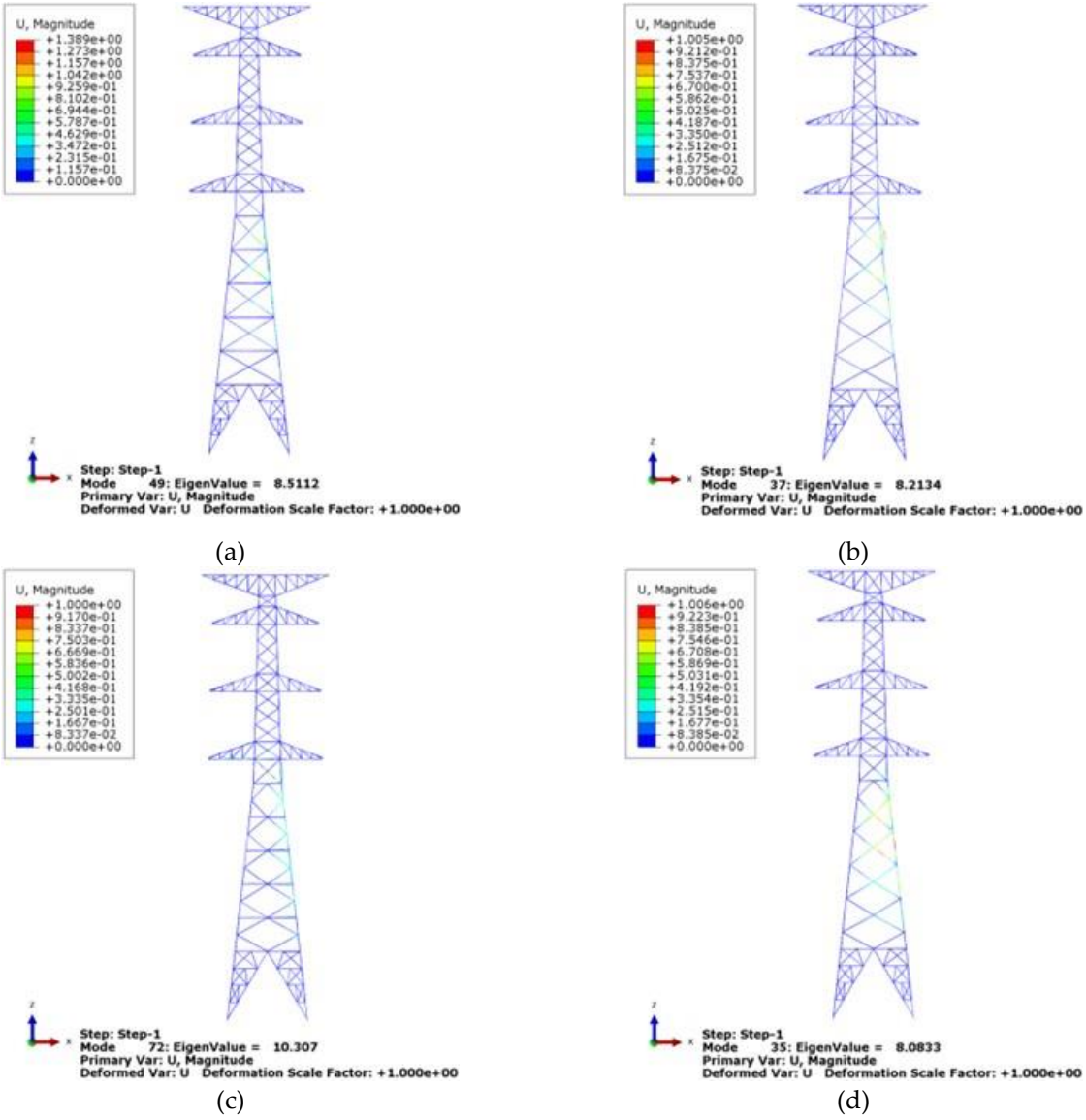

Figure 16. Eigenvalues and eigenmodes in the model with five equal braces: (a) Model with X braces and horizontal members; (b) Model with X braces without horizontal members; (c) Model with K braces and horizontal members; (d) Model with K braces without horizontal members

Preprints (www.preprints.org) | NOT PEER-REVIEWED | Posted: 7 December 2022 doi:10.20944/preprints202212.0129.v1

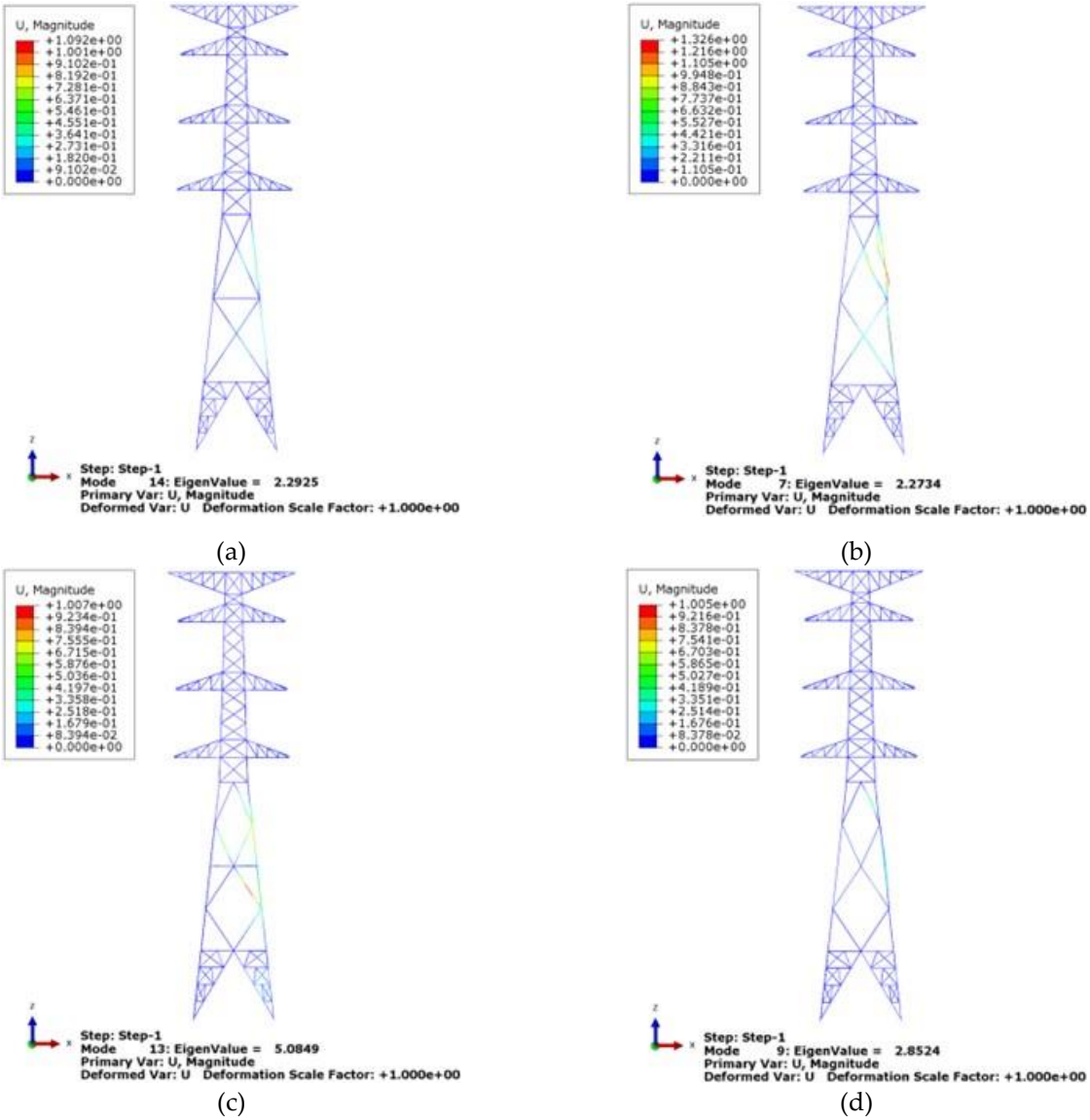

Figure 17. Eigenvalues and eigenmodes in the model with two equal braces: (a) Model with X braces and horizontal members; (b) Model with X braces without horizontal members; (c) Model with K braces and horizontal members; (d) Model with K braces without horizontal members

3.3 Effects of the secondary members on the load-carrying capacity

The initial imperfection was applied in the finite element models by many researchers to accurately confirm the buckling of the structures [40-43]. In this study, the initial imperfection is applied using the buckling mode generated in the structure through elastic buckling analysis. The geometric nonlinear and inelastic analysis was performed to determine the effects of the shape, spacing of the braces, and horizontal members on the ultimate behavior. Figs. 17 and 18 show the deformed shapes of the transmission towers, obtained by the geometric nonlinear and inelastic analysis. The figures clearly exhibit the gradual increase of the deformation of the structure as the external load increases. Because the geometric nonlinear and inelastic analysis was conducted, the ultimate behaviors of each tower could be investigated. According to the analysis results, yield and inelastic buckling of the main posts were clearly observed as the significant causes of the ultimate behavior of the examined transmission towers. The ultimate modes and failed members were different with respect to the details of the brace and horizontal members.

The displacement at two points was checked to present the load–displacement curves. The first point was the topmost section, where the maximum displacement occurs, and the second point was the section with maximum deformation. These two points are

 doi:10.20944/preprints202212.0129.v1

illustrated in Fig. 19. The maximum deformation occurred on the main post, except for the model with X bracing of two equal spacings, on which the point of maximum deformation was on the braces. The load-carrying capacity was determined using the load–displacement curve. The load–displacement curves affected by the bracing shape, spacing, and horizontal members are shown in Figs. 20–23. The y-axis represents the load proportionality factor (LPF), and the x-axis represents the displacement of the models. Hor in legend is horizontal members. The bending point of the load–displacement curve corresponds to the maximum LPF. The state of reaching the maximum LPF is defined as the limit state in this study. The maximum LPF of the models was compared to analyze the load-carrying capacity. Table 8 shows the maximum LPF of the models affected by the horizontal and brace members. In models with five equal bracings with a sufficiently low slenderness ratio, the stiffness of the main post and brace was sufficient to resist the load applied in the transmission tower. Therefore, the presence of horizontal members and the shape of brace members did not affect the results. However, as the slenderness ratio increased, the effects of the horizontal members depended on the brace shape. In the model with X bracing, the horizontal member is located in the section where the brace and main post are connected. Because the effective buckling length of the main post is not reduced even if the horizontal member is removed, the horizontal members do not affect the load-carrying capacity in the two equal-spacing models with large slenderness ratios. However, the horizontal member plays a role in reducing the effective buckling length of the main post in models with K bracing and enhances their load-carrying capacity. By analyzing the results of the geometric nonlinear and inelastic analysis, it was confirmed that the horizontal member has a limited effect on the load-carrying capacity. When the spacing of braces is decreased to increase the number of braces, there is little enhancement of the load-carrying capacity based on the effect of horizontal members. However, if K bracing is induced by the proper arrangement of horizontal members, the effective buckling length decreases, and the load-carrying capacity is limitedly enhanced in models with a large slenderness ratio. In addition, by increasing the spacing of the braces, the number of horizontal members was reduced, and the configuration of the transmission towers could be further simplified.

Preprints (www.preprints.org) | NOT PEER-REVIEWED | Posted: 7 December 2022 doi:10.20944/preprints202212.0129.v1

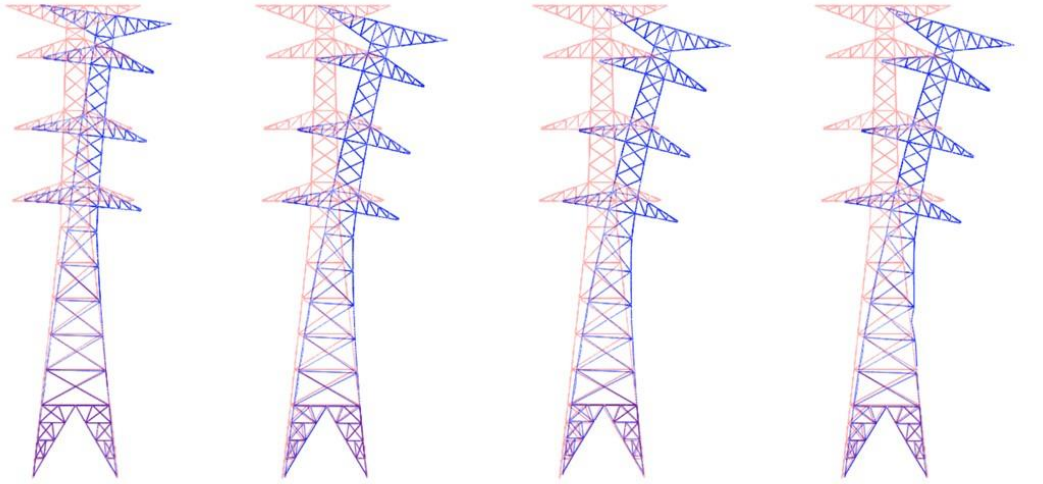

(a) LPF = 1.012 (b) LPF = 1.856 (c) LPF = 2.082 (d) LPF = 1.946 (in load decrease path)

(a)

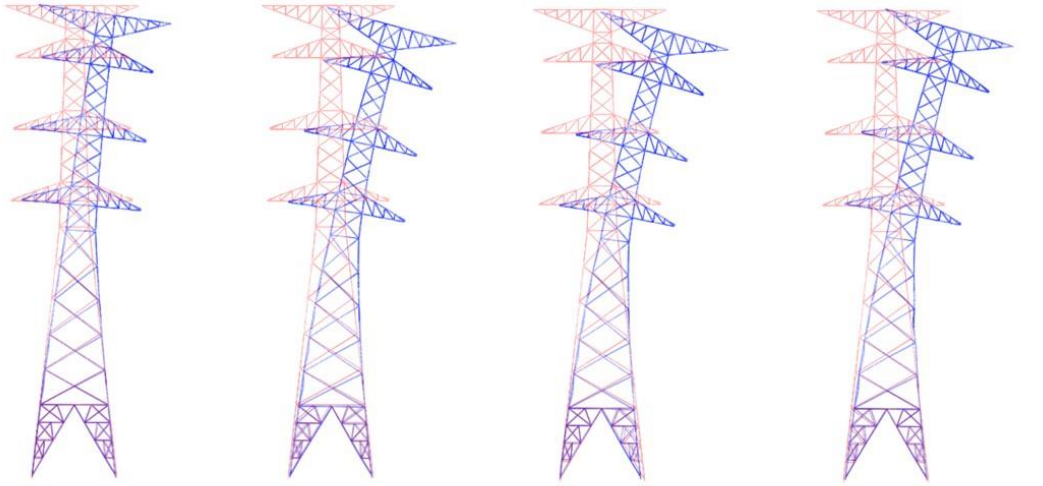

(a) LPF = 1.012 (b) LPF = 1.955 (c) LPF = 2.057 (d) LPF = 1.953 (in load decrease path)

(b)

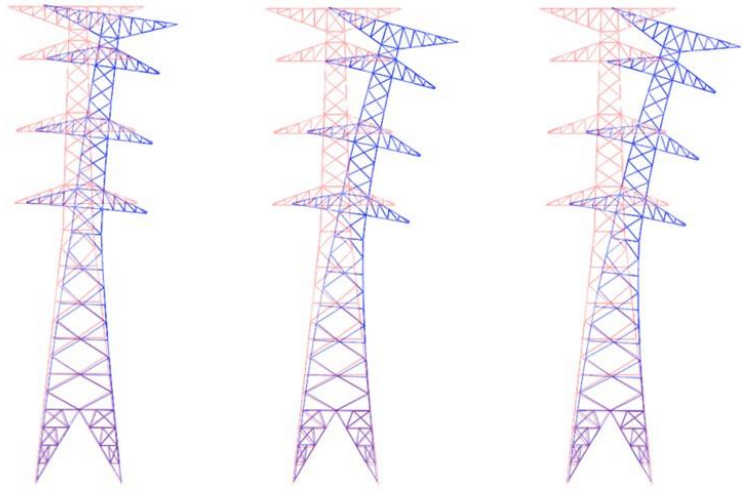

(a) LPF = 1.012 (b) LPF = 1.855 (c) LPF = 2.078

(c)

Preprints (www.preprints.org) | NOT PEER-REVIEWED | Posted: 7 December 2022 doi:10.20944/preprints202212.0129.v1

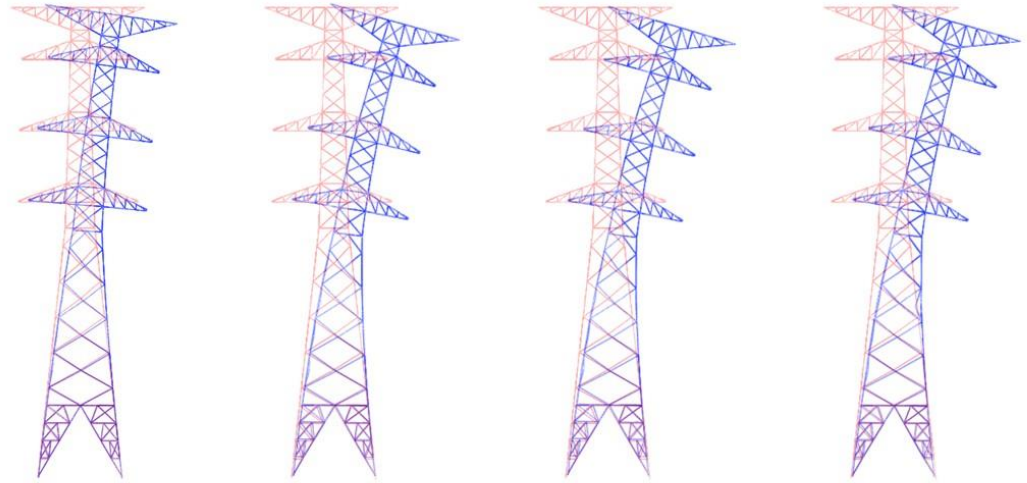

(d)

Figure 18. Progress in deformation of the transmission towers with five equal braces (scale factor 10.0): (a) Model with X braces and horizontal members; (b) Model with X braces without horizontal members; (c) Model with K braces and horizontal members; (d) Model with K braces without horizontal members

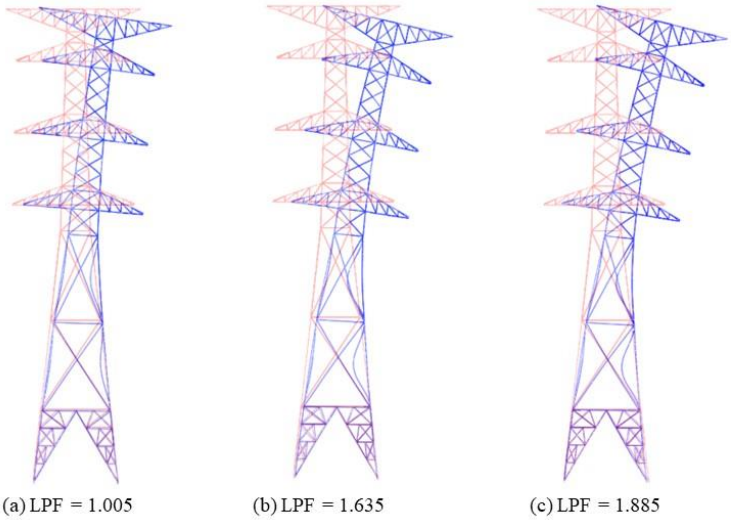

(a)

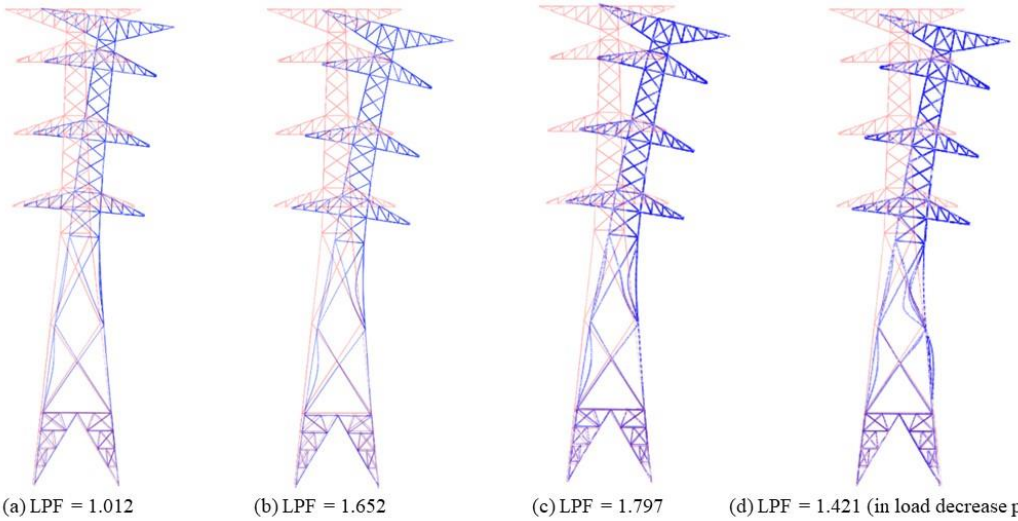

(b)

Preprints (www.preprints.org) | NOT PEER-REVIEWED | Posted: 7 December 2022 doi:10.20944/preprints202212.0129.v1

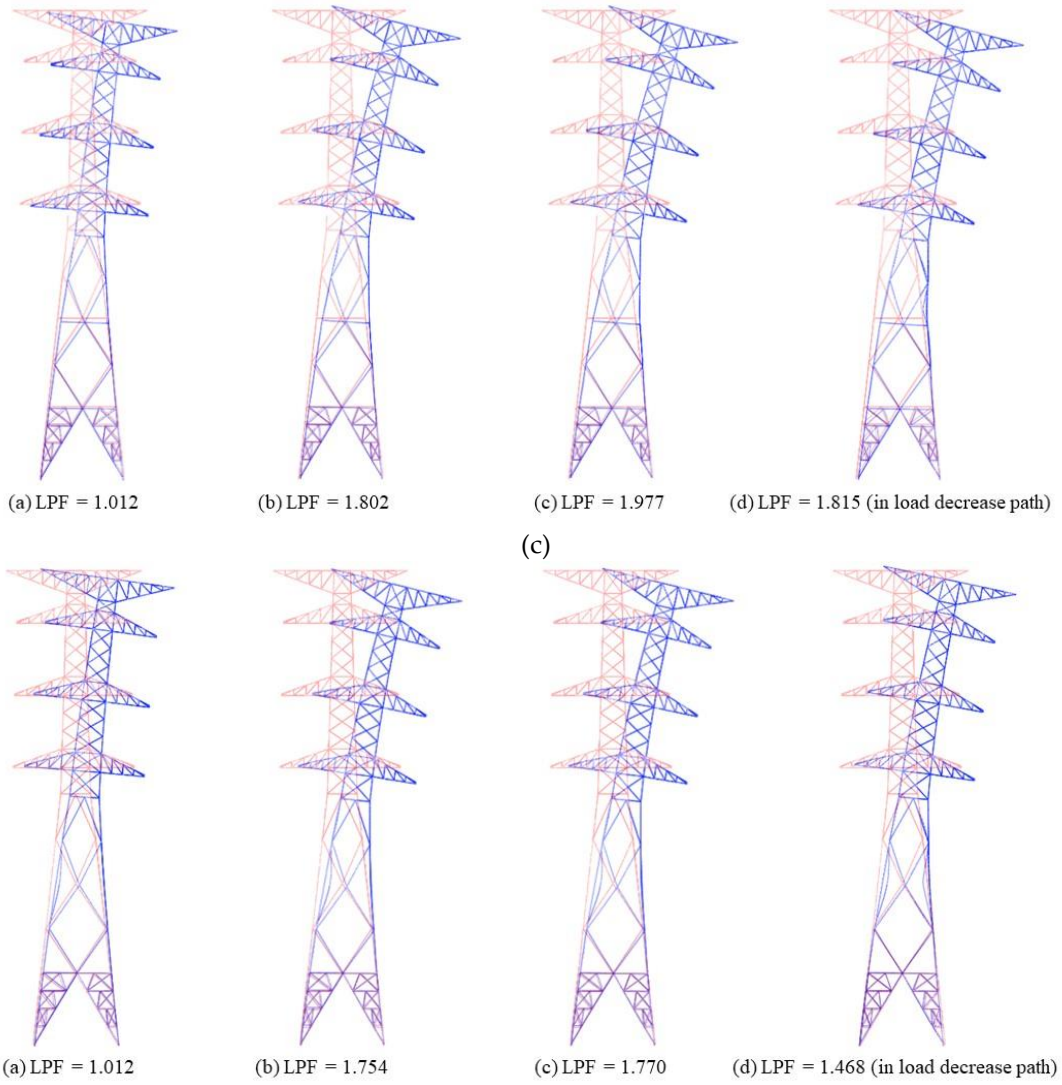

Figure 19. Progress in deformation of the transmission towers with two equal braces (scale factor 10.0): (a) Model with X braces and horizontal members; (b) Model with X braces without horizontal members; (c) Model with K braces and horizontal members; (d) Model with K braces without horizontal members

Preprints (www.preprints.org) | NOT PEER-REVIEWED | Posted: 7 December 2022 doi:10.20944/preprints202212.0129.v1

Table 8. Load-carrying capacity of models affected by parameters

Details	Models with X bracing		Models with K bracing	
	With horizontal members	Without horizontal members	With horizontal members	Without horizontal members
Five equal spacings of braces	2.082	2.057	2.078	2.060
Two equal spacings of braces	1.885	1.797	1.977	1.770

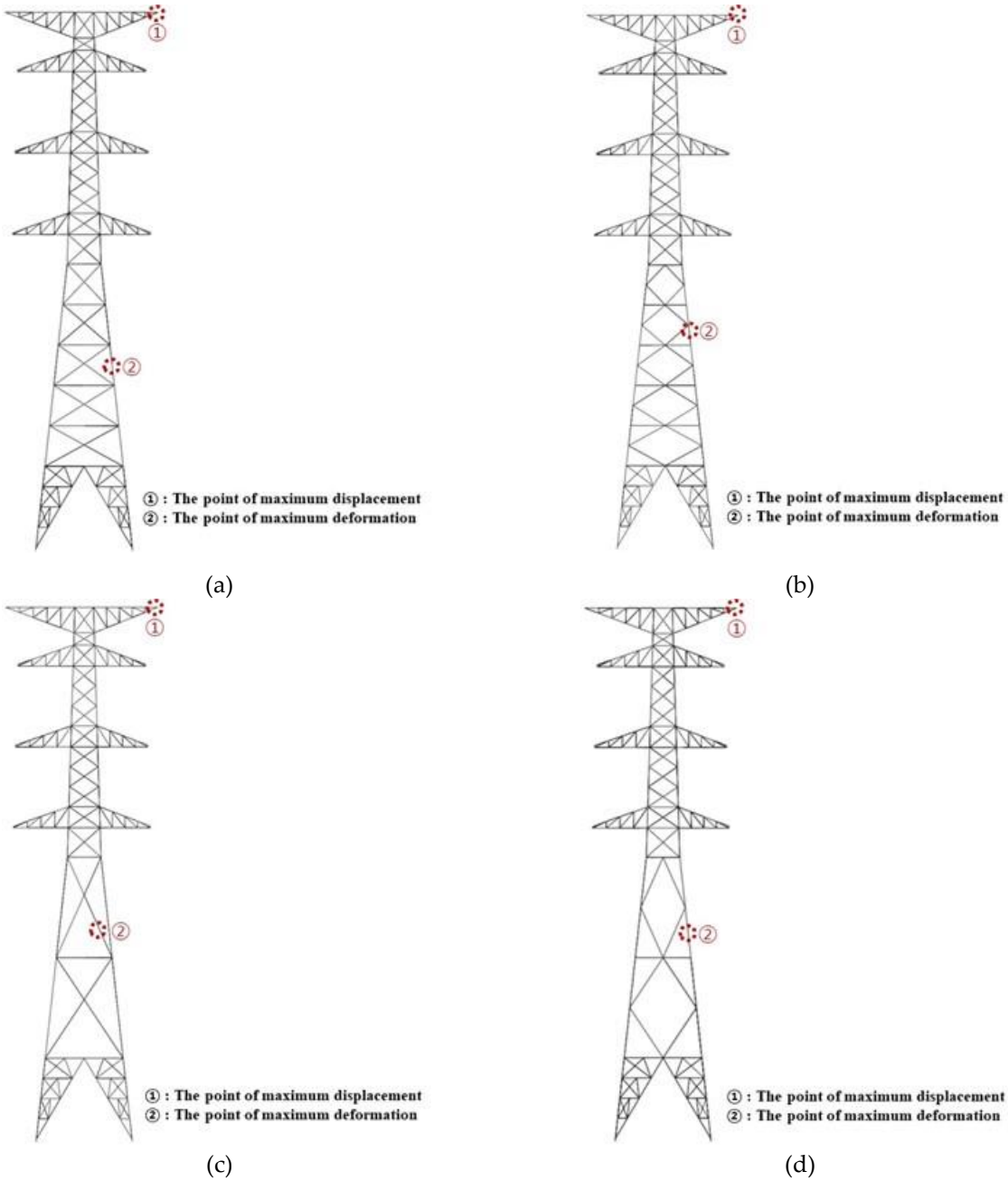

Figure 20. Two points to determine the load–displacement curve in the analytical models: (a) Model with X bracing of five equal spacings; (b) Model with K bracing of five equal spacings; (c) Model with X bracing of two equal spacings; (d) Model with K bracing of two equal spacings

Preprints (www.preprints.org) | NOT PEER-REVIEWED | Posted: 7 December 2022 doi:10.20944/preprints202212.0129.v1

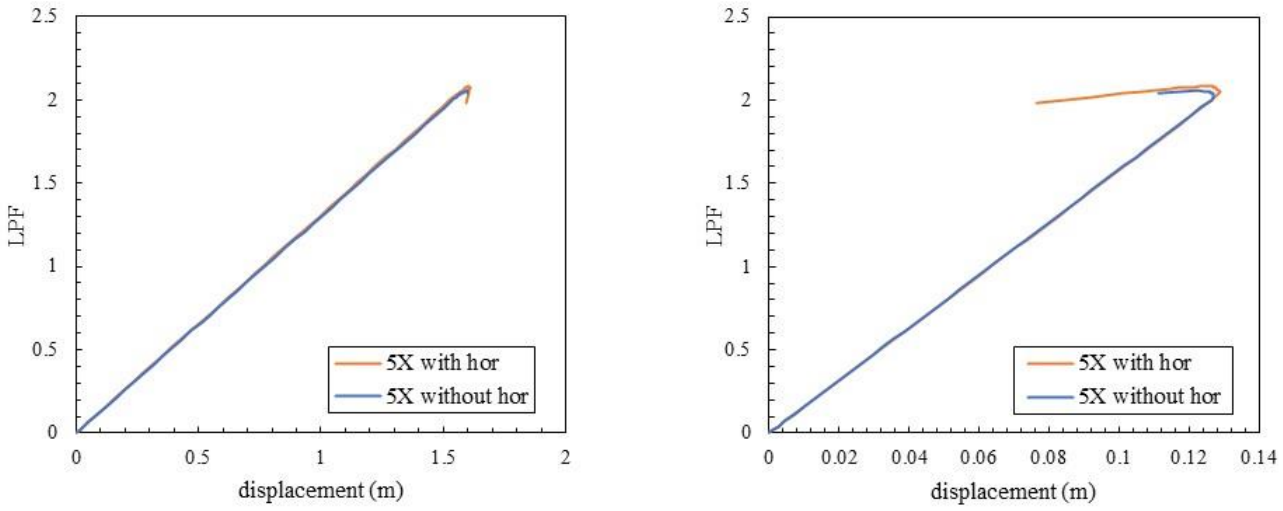

Figure 21. Comparison of load–displacement curves in models with five equal X braces with or without horizontal members; (a) Topmost section; (b) Section of the main post

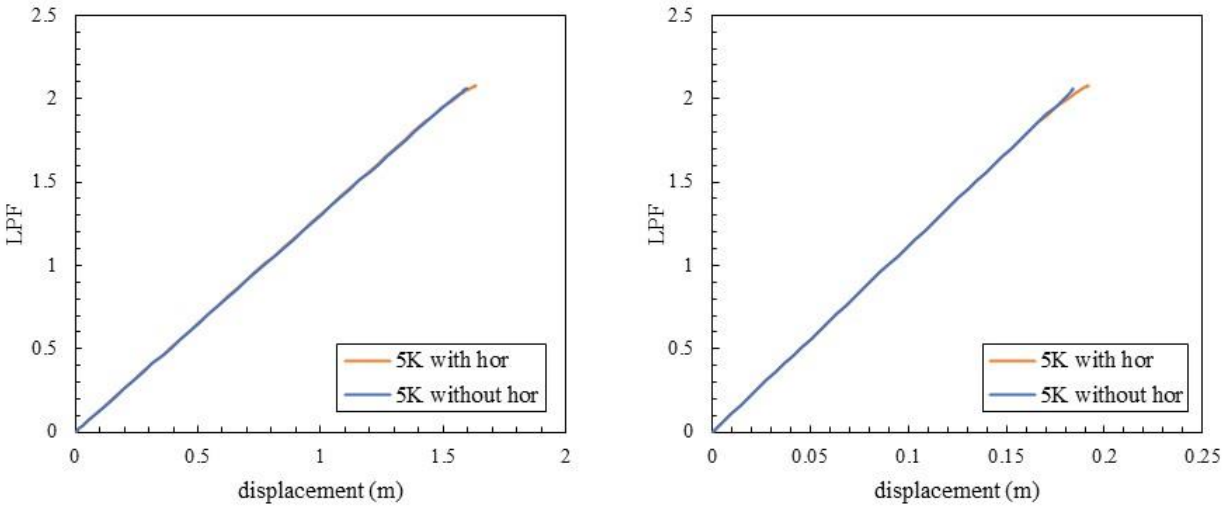

Figure 22. Comparison of load–displacement curves in models with five equal K braces with or without horizontal members; (a) Topmost section; (b) Section of the main post

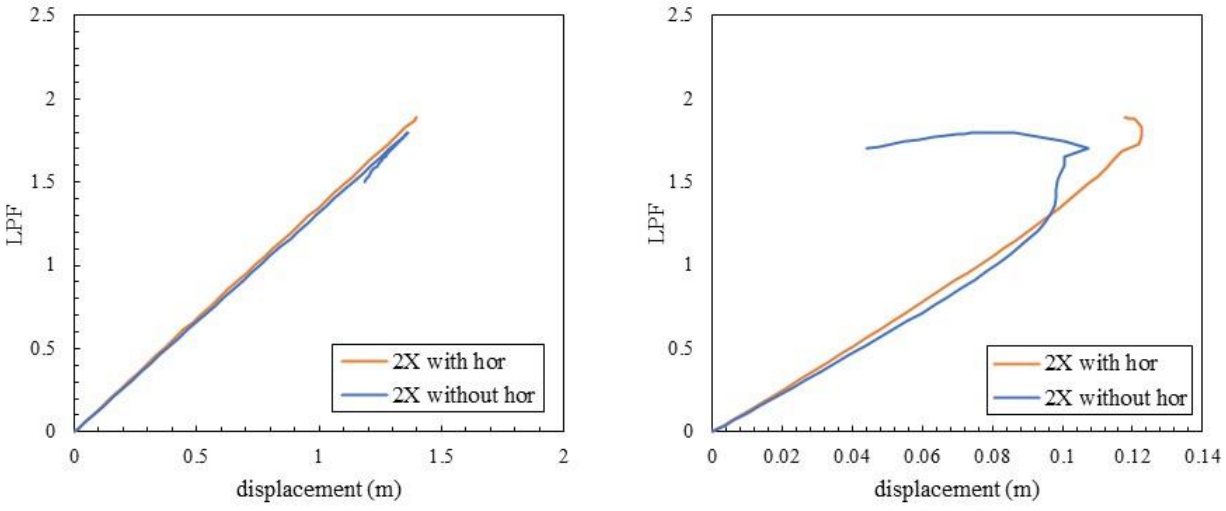

Preprints (www.preprints.org) | NOT PEER-REVIEWED | Posted: 7 December 2022 doi:10.20944/preprints202212.0129.v1

(a) (b)

Figure 23. Comparison of load–displacement curves in models with two equal X braces with or without horizontal members; (a) Topmost section; (b) Section of the brace

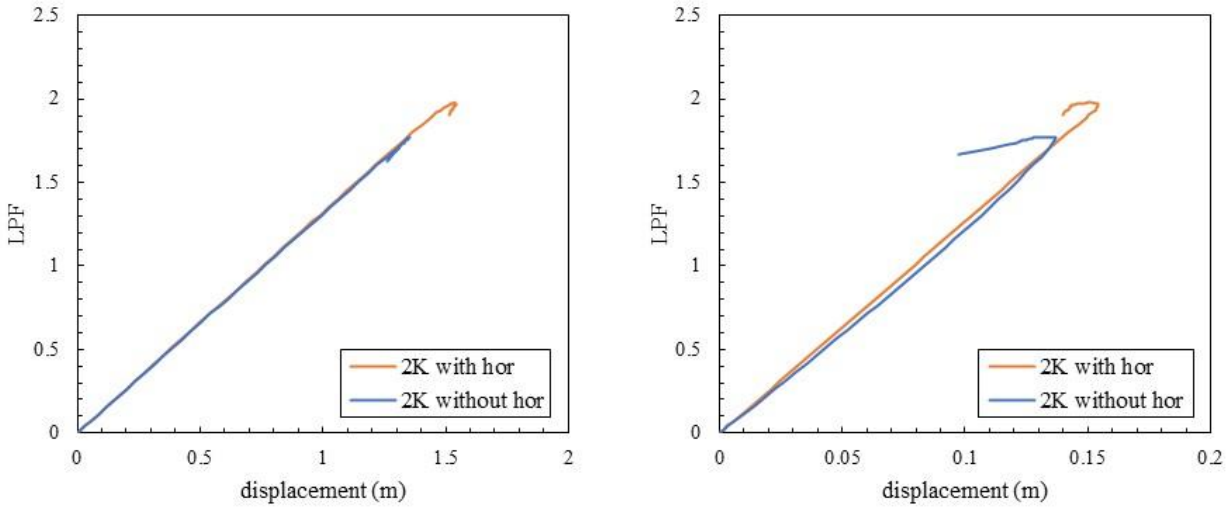

(a) (b)

Figure 24. Comparison of load–displacement curves in models with two equal K braces with or without horizontal members; (a) Topmost section; (b) Section of the brace

4. Conclusion

In this study, the effect of horizontal members on the overall behavior of large-capacity transmission towers was studied. In addition to horizontal members, the shape and spacing of braces, which could affect the overall behavior of the structure, was also studied. The following conclusions were reached by performing linear static, eigenvalue, and geometric material nonlinear analyses.

The linear static analysis confirmed that there was no significant effect of the horizontal members and braces on the displacement and distortion of the transmission tower when torsional loads were applied. Regardless of the presence of a horizontal member, the structural behaviors of the towers were nearly the same.

In the results of the eigenvalue analysis, an equal-spacing model with X bracing did not have an effect on the horizontal members. However, the spacing of the braces affected the eigenvalues. The brace spacing and horizontal members affected the results of the elastic buckling strength in the models with K bracing. As the slenderness ratio increased, the effect of the horizontal members increased. The horizontal members reduced the effective buckling length to effectively enhance the elastic buckling strength in K bracing.

By analyzing the load–displacement curve obtained by the geometric nonlinear and inelastic analysis, it was found that the load-carrying capacity in the model with X bracing is affected by the spacing of braces and is not affected by horizontal members. However, the effect of the horizontal members limitedly enhances the load-carrying capacity of models with K bracing and a large slenderness ratio. Bracing formation with a large slenderness ratio is effective to increase the load-carrying capacity. Furthermore, By increasing the spacing of the braces, the number of horizontal members can be reduced, and the members of the transmission towers could be simplified.

By comparing the results of the eigenvalue analysis and the geometric nonlinear and inelastic analysis, the ultimate strength was lower in the geometric nonlinear and inelastic analysis because the material features were reflected. In other words, material features were more dominant than geometric features in the analysis.

Based on the comparative study, it can be concluded that bracing directly affects the structural behavior and load-carrying capacity of the towers, while the effect of the horizontal members is limited. If the brace is sufficiently erected, the number of horizontal

 doi:10.20944/preprints202212.0129.v1

members can be significantly reduced so that the structural configuration can be simplified.

Author Contributions: Conceptualization, J.H.K. and S.K.; methodology, P.K., W.S.H., and S.K.; software, Y.J.K. and S.K.; validation, J.H.K. and S.K.; formal analysis, P.K. and W.S.H; investigation, P.K., W.S.H., and J.L.; resources, Y.J.K. and S.K.; data curation, P.K.; writing—original draft preparation, P.K.; writing—review and editing, J.L. and S.K.; visualization, P.K.; supervision, S.K.; project administration, J.H.K. and S.K.; funding acquisition, S.K. All authors have read and agreed to the published version of the manuscript." Please turn to the CRediT taxonomy for the term explanation. Authorship must be limited to those who have contributed substantially to the work reported.

Funding: This study was supported by the Korea Electric Power Research Institute (KEPRI) (CX72200091). In addition, this research was supported by a National Research Foundation of Korea (NRF) grant funded by the Korean government (MSIT) (No. NRF-2021R1A5A1032433).

Data Availability Statement: Data is contained within the article.

Acknowledgments: This study was supported by the Korea Electric Power Research Institute (KEPRI) (CX72200091). In addition, this research was supported by a National Research Foundation of Korea (NRF) grant funded by the Korean government (MSIT) (No. NRF-2021R1A5A1032433).

Conflicts of Interest: The authors declare no conflict of interest.

References

1. American Society of Civil Engineers, ASCE Manual 74, Guidelines for electrical transmission line structural loading fourth ed. ASCE, New York, 2020.
2. Dreyer, W. Special features in the design of transmission tower lines as imposed by electrical conditions, Trans. Am. Inst. Electr. Eng. XLII (1923) 962–966.
3. Taniwaki, K.; Ohkubo, S. Optimal synthesis method for transmission tower truss structures subjected to static and seismic loads, Struct. Multidisc. Optim. 26 (2004) 441–454.
4. Kaminski, J.; Riera , J.D.; de Menezes, R.C.R; Miguel, L.F.F. Model uncertainty in the assessment of transmission line towers subjected to cable rupture, Eng. Struct. 30 (2008) 2935–2944.
5. Ju, Y.Z.; Xue, Q.L.; Li, H. Failure analysis of transmission tower under the effect of ice-covered power transmission line, 2009 First International Conference on Information Science and Engineering, Nanjing, China, December 2009, 4301–4304. https://doi.org/10.1109/ICISE.2009.586.
6. Zheng, H.D.; Fan, J.; Long, X.H. Analysis of the seismic collapse of a high-rise power transmission tower structure, J. Constr. Steel Res.134 (2017) 180–193.
7. Cai, M.; Yang, X.; Huang, H.; Zhou, L. Investigation on galloping of d-shape iced 6-bundle conductors in transmission tower line, KSCE J Civ. Eng. 24 (2020) 1799–1809. http://doi.org/10.1007/s12205-020-0595-z.
8. Govindasamy, N.; Syamsir, A.; Mardi, N.H.; Malek, M.A. Effect of tsunami load by earthquake at manila trench on transmission tower, Ain Shams Eng. J. 12 (2021) 3593–3602.
9. Savory, E.; Parke, G.; Zeinoddini, M.; Toy, N.; Disney, P. Modelling of tornado and microburst-induced wind loading and failure of a lattice transmission tower, Eng. Struct. 23 (2001) 365–375.
10. Shehata, A.Y.; El Damatty, A.A.; Savory, E. Finite element modeling of transmission line under downburst wind loading, Finite Elem. Anal. Des. 42 (2005) 71-89.
11. Zhang, Z.; Li, H.; Li, G.; Wang, W.; Tian, L. The numerical analysis of transmission tower-line system wind-induced collapsed performance, Math. Probl. Eng. 2013 (2013), 413275. http://doi.org/10.1155/2013/413275.
12. Tian, L.; Zeng, Y. Parametric study on tuned mass dampers for long span transmission tower-line system under wind loads, Shock Vib. 2016 (2016), 4965056. http://doi.org/10.1155/2016/4965056.
13. Tapia-Hernandez, E.; Ibarra-González, S.; De-León-Escobedo, D. Collapse mechanisms of power towers under wind loading", Struct. Infrastruct. Eng. 13 (2017) 766–782
14. Tian, L.; Pan, H.; Qui, C.; Ma, R.; Yu, Q. Wind-induced collapse analysis of long-span transmission tower-line system considering the member buckling effect, Adv. Struct. Eng. 22 (2019) 30–41.

15. Yang, X.; Lei, Y.; Liu, L.; Huang, J. Simulation of nonstationary wind in one-spatial dimension with time-varying coherence by wavenumber-frequency spectrum and application to transmission line, Struct. Eng. Mech. 75 (2020) 425–434.
16. Tian, L.; Dong, X.; Pan, H.; Gao, G.; Xin, A. Critical seismic incidence angle of transmission tower based on shaking table tests, Struct. Eng. Mech. 76 (2020) 251–267.
17. Tapia-Hernandez, E.; De-Leon-Escobedo, D. Vulnerability of transmission towers under intense wind loads, Struct. Infrastruct. Eng. 2022 (2022), 18(9). 1235-1250. http://doi.org/10.1080/15732479.2021.1894183.
18. Prasad Rao, N.; Samuel Knight, G.M.; Lakshmanan, N.; Lyer, N.R. Investigation of transmission line tower failures, Eng. Fail. Anal. 17 (2010) 1127–1141.
19. Prasad Rao, N.; Samuel Knight, G.M.; Mohan, S.J.; Lakshmanan, N. Studies on failure of transmission line towers in testing, Eng. Struct. 35 (2012) 55–70.
20. Zhang, Z.; Xie, Q. Failure analysis of transmission tower subjected to strong wind load, J. Constr. Steel Res. 160 (2019) 271–279.
21. Albermani, F.G.A.; Kitipornchai, S. Numerical simulation of structural behaviour of transmission towers, Thin-Walled Struct. 41 (2003) 167–177.
22. Albermani, F.G.A.; Mahendran, M.; Kitipornchai, S. Upgrading of transmission towers using a diaphragm bracing system, Eng. Struct. 26 (2004) 735-744.
23. Xie, Q.; Sun, L. Failure mechanism and retrofitting strategy of transmission tower structures under ice load, J. Constr. Steel Res. 74 (2012) 26–36. https://doi.org/10.1016/j.jcsr.2012.02.003.
24. Xie, Q.; Sun, L. Experimental study on the mechanical behavior and failure mechanism of a latticed steel transmission tower, J. Struct. Eng. 139.6 (2013). 1009-1018. https://doi.org/10.1061/(ASCE)ST.1943-541X.0000722.
25. Cai, Y.; Xie, Q.; Xue, S. Effects of additional diaphragms on the wind-resistant performance of power transmission tower. 2016 World Congress on Advances in Civil, Environmental, and Materials Research (ACEM16). Jeju Island, Korea, August-September 2016.
26. Chen, J.; Cao, S.; Xian, Q. Design of the submerged floating tunnel operating under various conditions, IOP Conf. Ser.: Mater. Sci. Eng. 473 (2019), Seoul, South Korea.
27. Mahamid, M.; Tasbahji, T.; Tort, C. Investigating different horizontal bracing schemes on the deflection and behavior of latticed steel transmission line towers, Structures Congress, Orlando, USA, April 2019, 299–308. https://doi.org/10.1061/9780784482230.029.
28. Meshmesha, H.M.; Kennedy, J.B.; Sennah, K.; Moradi, S. Static and dynamic analysis of guyed steel lattice towers, Struct. Eng. Mech. 69 (2019) 567–577.
29. Sheppard, D.J.; Palmer, A.C. Optimal design of transmission towers by dynamic programming. Comput. Struct. 2 (1972) 455–468.
30. Natarajan, K.; Santhakumar, A.R. Reliability-based optimization of transmission line towers, Comput. Struct, 55 (1995) 387–403.
31. Mathakari, S.; Gardoni, P.; Agarwal, P.; Raich, A.; Haukaas, T. Reliability-based optimal design of electrical transmission towers using multi-objective genetic algorithms, Comput. Aided Civ. Infrastruct. Eng. 22 (2007) 282–292.
32. de Souza, R.R.; Fadel Miguel, L.F.; Lopez, R.H.; Miguel, L.F.F.; Torii, A.J. A procedure for the size, shape and topology optimization of transmission line tower structures, Eng. Struct. 111 (2016) 162–184.
33. Srihitha, S.; Rao, B.C.M. Analysis of transmission towers for optimal bracing configuration, J. Struct. Eng. 5 (2016), 1.
34. Taheri, F.; Ghasemi, M.R.; Dizangian, B. Practical optimization of power transmission towers using the RBF-based ABC algorithm, Struct. Eng. Mech. 73 (2020) 463–479.
35. Khodzhaiev, M.; Reuter, U. Optimization design of transmission tower based on intelligent selection, Eng. Struct. 240 (2021), 112306.
36. Grzywinski, M. Optimization of spatial truss towers based on Rao algorithms, Struct. Eng. Mech. 81 (2022) 367–378.
37. American Society of Civil Engineers, Design of latticed steel transmission structure. ASCE, New York, 2015.
38. Albermani, F.G.A.; Kitipornchai, S. Nonlinear analysis of thin-walled structures using least element/member, Eng. Struct. 116 (1) (1990) 215-234.
39. Kroeker, D. Structural analysis of transmission towers with connection slip modeling. Master' Thesis, University of Manitoba, Winnipeg, Canada, 2000
40. Jeddi, A. B., Shafieezadeh, A., Hur, J., Ha, J. G., Hahm, D., & Kim, M. K. Multi-hazard typhoon and earthquake collapse fragility models for transmission towers: An active learning reliability approach using gradient boosting classifiers. Earthquake Engineering & Structural Dynamics, 51(15), (2022)3552-3573.
41. Uriz, P., Filippou, F. C., & Mahin, S. A. Model for cyclic inelastic buckling of steel braces. Journal of structural engineering, 134(4), (2008) 619-628. ffect of modelling complexities on extreme wind hazard performance of steel lattice transmission-towers
42. Mohammadi Darestani, Yousef, Abdollah Shafieezadeh, and Kyunghwa Cha. "Effect of modelling complexities on extreme wind hazard performance of steel lattice transmission towers." Structure and Infrastructure Engineering 16.6 (2020): 898-915.
43. Wang, J., Li, H. N., Fu, X., Li, Q. Geometric imperfections and ultimate capacity analysis of a steel lattice transmission tower. Journal of Constructional Steel Research, (2021). 183, 106734.